Noble Nanofluids and Their Hybrids for Heat Transfer

Subjects: Energy & Fuels

Contributor: José Pereira , Ana Moita , António Moreira

The novel class of fluids known by nanofluids is composed of colloidal suspensions of solid nanoparticles dispersed in a base fluid. When the solid nanoparticles are made of noble metals they can be named as noble metals nanofluids or noble nanofluids for short.

noble metals heat transfer nanofluids thermal management

1. Introduction

The nanotechnology area is one of the most dynamic research areas in the materials science and technology and the production of nanoparticles is gaining an ever-increasing worldwide importance. The nanoparticles show improved properties that are influenced by their characteristics like shape, size, and nature. The nanoparticles can be divided into inorganic and organic. The inorganic nanoparticles incorporate semi-conductor nanoparticles, metallic nanoparticles like gold, silver, and copper, and magnetic nanoparticles like cobalt and iron, whereas the organic nanoparticles category incorporates carbon nanoparticles like, for instance, carbon nanotubes.

There is a growing enthusiasm for noble metal nanoparticles and nanofluids like the ones of gold, silver, platinum, palladium, and ruthenium, given that they offer superior thermophysical properties together with advantageous features that are not easily encountered in other nanoparticles like biocompatibility, non-cytotoxicity, and chemical inertness [1]. Together with the increasing use of the noble metal nanofluids came the exploration of bio-friendly synthesis methods. The implementation of the green synthesis of the noble metals nanoparticles and nanofluids is still advancing as a key branch of nanotechnology where the use of plant extracts and biomass, and microorganisms for the generation of nanoparticles could be a reasonable option for chemical and physical methods processed in a bio-friendly mode. The green synthesis progress over the conventional physical and chemical procedures is that the green procedures are environment friendly, cost-effective, and easily scalable for vast scale production of nanoparticles and nanofluids, whereas the limitations originated from the high-temperature, energy, pressure, and toxic chemicals issues are not considered in the green synthesis [2].

The silver nanoparticles, for example, exhibit a considerable surface area that imparts to them remarkable catalytic activity and biochemical reactivity in comparison with larger nanoparticles with similar chemical composition. Moreover, the production of silver nanoparticles has attracted notorious attention due to the promising use in catalysis, plasmonic, antimicrobial activity [3], DNA sequencing, energy conversion, and biomedical applications [4]. The most common bottom-up method is the chemical reduction for the synthesis of silver nanoparticles [5]. Different

inorganic and organic reducing agents included in aqueous/non-aqueous solutions are normally employed for the silver ions reduction. Capping agents are additionally used for size stabilization of the nanoparticles.

A considerable amount of experimental and theoretical research was carried out to infer the effect of metal and metal oxide nanoparticles in the thermal conductivity enhancement of the nanofluids. It was found that a high thermal conductivity enhancement could be attained with noble metals nanofluids, even with very small concentrations of nanoparticles. Also, the heat transfer capability of the nanofluids with noble metals nanoparticles was reported to be much higher than the one, for example, of the metal oxide nanoparticles. The noble metals nanofluids were investigated by several researchers like, for instance, Salehi et al. [6] and Liu et al. [7] and they confirmed significant heat transfer improvements.

The main heat transfer application of the noble metals nanofluids is their use as the operating heat transfer media in the direct absorption solar collectors to improve the solar–thermal conversion efficiency. The common solar collectors pose the question on how to ameliorate the absorption efficiency of solar energy and how to efficiently transmit the absorbed energy in the working medium. With enhanced absorption and heat transfer characteristics, the noble metal nanofluids can accomplish the requirements for the working thermal fluid in solar collectors, and greatly increase the conversion efficiency. In this sense, the researchers Neumann et al. [8] investigated that the gold nanofluids could generate vapor under concentrated sunlight irradiation. The research work indicated that 80% of the gold nanofluids that absorbed solar energy were directed to the vapor generation, but only approximately 20% of that was explored to enhance the temperature. It was believed that the thermal trapping action of the nanoparticles provoked a non-uniform distribution of temperature and the overheating in the nanofluids. Furthermore, the authors Otanicar et al. [9] investigated the absorption capability of the hybrid nanofluids composed of gold-iridium tin oxide nanostructures dispersed in Duratherm S flowing in the receiver of a photovoltaic/thermal solar parabolic trough collector at temperature values superior to 100 °C. The system showed better thermal characteristics in reference to the base fluid and achieved a photovoltaic efficiency of 4%, whilst attaining a peak thermal efficiency of 61% with an outlet temperature of the fluid of 110 °C.

Despite the improved heat transfer and energy absorption characteristics of the nanofluids, they may still pose threats to humans. Specifically, a great number of nanoparticles will migrate during the vapor generation under concentrated sunlight process of the nanofluids, which deserves more attention. In the last decades, the investigators have begun to dedicate time to the expected hazardous effects of rapidly developing nanoparticles and issued a first warning about the nanoparticles driven pollution [10]. Many works have reported that the nanofluids, including the metallic and carbon-based ones, had negative impact on humans, plants, and microorganisms [11]. Thus, it is paramount to deeply analyze the migration characteristics of the nanoparticles in vapor processes.

2. Heat Transfer Mechanisms and Influencing Factors

The heat transfer performance of the noble metals nanofluids can be affected by various factors and mechanisms. The most highlighted in the temperature are the effects of the solid-liquid interface Layer and interactions between

the Molecules of the metallic Nanoparticles and the Molecules of base fluid. Some of these effects that influence the heat transfer of the noble metals nanofluids are the aggregation morphology of the incorporated nanoparticles and the match degree of the phonon density of state. The aggregation morphology influence was already numerically addressed by the authors Du et al. [12], Song et al. [13], and Wang et al. [14][15]. The aggregation was simulated in Molecular Dynamics by a diffusion-limit-cluster-aggregation model, where the influence of the size of the nanoparticle, concentration, and number in a cluster on the aggregation structure were evaluated. The researchers concluded that at a fixed volumetric concentration and size of the included nanoparticles, the thermal conductivity of the metallic nanofluids increased linearly with decreasing fractal dimension of the aggregation. The authors interpreted the fact based on the more direct heat transfer channels between the nanoparticles and on the larger interface between the nanoparticles and the base fluid produced by a lower fractal dimension. Also, the results showed that the nanoparticle aggregation can dramatically increase the thermal conductivity of the nanofluids, and the aggregation can be more influent for smaller nanoparticles and lower concentrations. The main mechanism is that the aggregation raises the phonon mean free path in the solid phase, which further results in the thermal conductivity enhancement of the nanoparticles and nanofluids. Additionally, the authors Jin et al. [16] examined if nanoparticle additions with higher thermal conductivity are necessary for greater thermal conductivity of nanofluids and studied gold-water, silver-water, copper-water, and iron-water nanofluids by the dynamic molecular method. The results showed that the gold-water nanofluid exhibited the highest thermal conductivity and thicker nanolayer because of the stronger interaction forces between the gold and water molecules. Also, the authors proposed an index designated by match degree of phonon density of state and argued that the phonon match between the molecules of the metal and water molecules was the critical underlying mechanism for the thermal conductivity enhancement of the metal-water nanofluids. Moreover, the researchers Cui et al. [17] proposed to add Janus nanoparticles into a fluid commonly named as Janus nanofluids, to further increase the thermal conductivity of the nanofluids. Through molecular dynamics simulations, the authors reported that the thermal conductivity can be appreciably improved by the incorporation of Janus nanoparticles into the base fluids in contrast with the traditional nanofluids. Based on the determination of the molecular radial distribution function around the added nanoparticles, and the diffusion coefficients of the base fluid and the Janus nanoparticles, the thermal conductivity improvement in the Janus nanoparticles containing nanofluids was attributed to the increased Brownian motion of the Janus nanoparticles that augments the likelihood of more inter-molecular collisions and enhances the heat transfer capability of the medium. Answering to the question of why can hybrid nanofluid improve thermal conductivity more, the authors Guan et al. [18] evaluated the microscopic mechanism responsible for the enhancement in the thermal conductivity of hybrid nanofluids. The thermal conductivity and diffusion coefficient of copper-silver/argon hybrid nanofluid were estimated by molecular dynamics and the obtained results indicate that the peak enhancement in the thermal conductivity of nearly 70% was attained achieved for a hybrid nanofluid with copper-silver 50:50%/argon that was much larger than the around 48% and 26.4% achieved for the silver/argon and copper/argon nanofluids. The radial distribution function demonstrates that the atoms of argon on the surface of the nanoparticles are in dynamical equilibrium. The nanolayer densities and diffusion coefficients are calculated for various hybrid nanofluids to explain the underlying mechanism of the enhancement in the thermal conductivity. The consistency of the thermal conductivity with the nanolayer density and diffusion coefficient indicates that nanolayer structure and diffusion of the argon are the two underneath mechanisms. The authors

stated that the nanolayer around nanoparticles can enhance the heat conductance of the nanofluid due to the greater density and the ordered structure of nanofluid may result in more interactions between the molecules of the nanoparticles and the molecules of the base fluid. Hence, a greater density of nanoparticles will conduct to a greater density of nanolayer. Nonetheless, the surface structure of the nanoparticles could be even more relevant than the density of the nanoparticles, given that it was found that the nanofluids having diverse hybridization ratios possessed different thermal conductivity. Also, the copper-silver 50:50%/argon nanofluid exhibited the highest nanolayer density and diffusion coefficient in respect to those of the nanofluids with smaller or greater hybridization ratios. The reasons are that the copper-silver 50:50%/argon nanofluid had the most lattice distortions on the surface of the nanoparticles, resulting in a greater polarization and interaction of dipoles, being the lightest copper-silver 50:50% nanoparticle capable of inducing the greatest Brownian motion. Moreover, the motion of the base fluid molecules in the nanolayer and the diffusion coefficient can also influence the heat transfer capability of the nanofluid.

3. Noble Nanofluids

3.1. Gold Nanofluids

The gold nanoparticles possess the benefits of being biocompatible and non-cytotoxic. Besides, gold has been used internally in humans for the last five or six decades because of their chemical inertness. The gold nanoparticles dimensions can be minimized during their synthesis and functionalization. The gold aqueous nanofluids using molecular dynamics nanofluids are included in a novel class of fluids with superior thermophysical characteristics and heat transfer behavior. In this sense, the researchers Zhang et al. [19] observed that the gold nanofluids exhibited enhanced solar thermal conversion. The authors observed that at only 0.15% wt., the gold nanofluids enhanced the photothermal conversion efficiency by 20%. Additionally, the authors Sabir et al. [20] evaluated the heat transfer performance of gold aqueous nanofluids under laminar flow and imposed fixed heat flux flowing in a heat pipe. The obtained results demonstrated increases in the Heat Transfer Coefficient (HTC) of 8%, 15%, and 23% at the minimal volumetric concentrations of 0.00015% vol., 0.00045% vol., and 0.000667% vol. of gold nanoparticles, respectively, in reference to that of the water itself. The authors observed also that the heat transfer enhancement was higher in the inlet nearby area and the thermal boundary layer of the nanofluids was superior to the one of the water alone. The researchers concluded that the gold nanofluids are very suitable for heat transfer purposes in micro processes using heat pipes. The governing mechanisms of the heat transfer enhancement rely on factors like the enhanced thermal conductivity, viscosity, and nanoparticle Brownian motion and migration. Besides, the authors Chen et al. [21] inferred the impact of the size of the gold nanoparticles on the photothermal conversion efficiency in cube and flat direct absorption solar collectors. The nanoparticles were manufactured by a seed mediated method and the experimental results showed that the gold nanofluids at 0.000008% wt. provided photothermal conversion efficiencies enhancements of nearly 21.3% and 20% for flat shaped and cube-shaped direct absorption solar collectors, respectively, in reference to that of the water itself. The cube-shaped collector presented a greater photothermal conversion efficiency than the one attained with the flat-shaped collector operating with the same nanofluids, given that the cube-shaped collector optical path length was

superior to the same length of the flat-shaped collector and, consequently, the former had an enhanced solar radiation absorption. The photothermal conversion efficiency diminished with increasing size of the gold nanoparticles for the flat-shaped collector because of the interactions of the optical properties of the nanofluids, heat losses to the surrounding environment, and thermal conductivity increase. Nonetheless, the influence of the size of the gold nanoparticles on the cube-shaped collector was not so evident as it happens in the flat-shaped collector. Besides, the authors Burgos et al. [22] evaluated the impact of the concentration and dimensions of the gold nanoparticles dispersed in water on the parameters of a direct absorption solar collector, such as the stability of the nanofluids, extinction coefficient, and photothermal efficiency. The sizes of the nanoparticles were of 5 nm and 20 nm and their concentrations were of around 5 ppm, 28 ppm, and 51 ppm. The authors demonstrated that the incorporation of gold nanoparticles with a surface plasmon resonance of 516 nm for the 5 nm-sized particles and of 520 nm for the 20 nm-sized particles enhanced considerably the light absorption capacity of the water itself. Also, the research team confirmed that the photothermal conversion efficiency was closely linked with the concentration and size of the dispersed nanoparticles. In addition, the photothermal conversion efficiency was increased to a maximum 121% in comparison with that of the water alone using the 5 nm-sized gold nanoparticles at 51 ppm. Also, the authors reported that the photothermal conversion efficiency increase within the employed concentration range did not follow a linear relationship, given that it was a threshold beyond which no further increase was observed. The results demonstrated the beneficial features of using smaller sized gold nanoparticles at lower concentrations in solar collectors. One of them is the ability to reduce the needed thermal fluid overall volume to reduce the collector depth. This will lead to smaller and less costly direct absorption solar collectors. Moreover, the researchers Lopez-Munoz et al. [23] examined the influence of the size, concentration, and base fluid on the thermal diffusivity of urchin-like gold nanofluids produced by a hydroquinone two-step method using a seed-mediated growth. The urchin-like gold nanoparticles low size dispersion synthesized by this methodology was found to be advantageous in comparison with the single-step methodology, which are not so able for controlling the dimensions of the branched nanoparticles. This tuning capability is vital since it is closely linked to the adjustable surface plasmon resonance of the urchin-like gold nanoparticles. The research team observed that the thermal diffusivity ratio altered inversely with the size of the nanoparticles that was between 55 nm and 115 nm. Also, the thermal diffusivity ratio augmented with increasing concentration of nanoparticles and decreasing thermal diffusivity of the base fluid. Besides, the researchers Carrilo-Berdugo et al. [24]. It was experimentally found that a concentration of 0.01% wt. of gold nanoplates provided a 1.6% increase in the specific heat capacity and an enhancement of around 18% in the thermal conductivity at 373 K. The gold nanofluids had a eutectic mixture of biphenyl and diphenyl oxide for base fluid, which is commonly employed in concentrated solar power stations. The research team verified that at 4.8% wt. of gold nanoplates and at 373 K, the thermal conductivity and specific heat increased by nearly 25% and 6%, respectively. The obtained results showed that the alteration degree of these properties depended on the surface chemistry of the nanomaterial. Also, the density functional theory simulations revealed that a layer of physiosorbed diphenyl oxide and biphenyl molecules were formed onto the gold surfaces. The molecular dynamics simulations aided to achieve a correlation between the interactions at the interface and the thermophysical features of the nanofluids. Henceforth, it can already be stated that higher specific heat capacity increases and lower high-temperature thermal conductivity increases can be obtained with more intense interactions between the existing molecules at the solid–liquid interfaces. Besides, the authors Han et al. [25]

introduced an optimization procedure to evaluate the impact of the concentration and size of the nanoparticles, and optical thickness of gold nanofluids filtered photovoltaic/thermal systems including silicon solar cells. The surface modified gold-water and gold-ethylene glycol nanofluids with polyvinylpyrrolidone or polyethylene glycol were synthesized to act as an optical filter for photovoltaic/thermal systems. Also, prolonged storage, heating at high temperature values, and cycles of solar irradiation under flowing conditions experiments were performed to prove the stability over time of the surface modified gold nanoparticles. Additionally, there were also carried out indoor flowing tests to evaluate the effectiveness of the gold polyvinylpyrrolidone modified-ethylene glycol nanofluid filter. The obtained results indicated that a 1.37 merit function maximum for a photovoltaic/thermal system with a gold aqueous nanofluid filter was attained at 49 ppm with 20 mm of optical thickness and 20 nm of average nanoparticle size. In addition, the achieved merit function value for the best gold/water nanofluid filtered photovoltaic/thermal system was superior to that encountered in the literature, demonstrating the improved reliability and applicability of the optimization methodology followed by the authors. The prepared gold nanoparticles with 20 nm of average size and good distribution showed superior optical characteristics, being the localized surface plasmon resonance peak at 525 nm. In view of the stability experimental tests, the coated gold nanoparticles with polyvinylpyrrolidone or polyethylene glycol extended their dispersion stability over time. The absorbance of gold dispersed in polyvinylpyrrolidone/ethylene glycol nanofluids after 10 h of heating at a temperature of 110 °C exhibited only a negligible alteration. Apart from this, the plasmonic peak of the gold polyvinylpyrrolidone modified nanoparticles portrayed a slight enhancement after four cycles of irradiation and flowing. Additionally, the polyvinylpyrrolidone was a better protective shell for the gold nanoparticles in comparison to the polyethylene glycol. The results of the flowing tests indicated that the mass flow rate affected only slightly the photo-electrical conversion capability of the silicon solar cell, but it negatively affected the efficiency of the gold-polyvinylpyrrolidone-ethylene glycol nanofluids filtered photovoltaic/thermal system. For the photovoltaic/thermal system at 29 ppm of gold-polyvinylpyrrolidone-ethylene glycol nanofluid filter, the efficiency decreased from nearly 60% to 54% in the case where the mass flow rate increased from 2 mL/min to 6 mL/min. The photovoltaic/thermal system using the 29-ppm gold-ethylene glycol nanofluid filter with a mass flow rate of 2 mL/min attained a merit function value, photoelectrical efficiency, photothermal efficiency, and exergy efficiency of 1.95, 9.6%, 60.2%, and 14%, respectively. Furthermore, the authors Amjad et al. [26] performed an innovative experiment employing a single uniform solar heating system under 280 Suns of concentrated solar flux to evaluate the steam production capability of gold aqueous nanofluids. The researchers observed a non-uniform temperature distribution along the nanofluids heating path and proposed an integration method to determine the contribution of the sensible heating. Also, the researchers identified different stages of heating, which were the saturated boiling, and the surface and subcooled heating. In the surface heating, a large energy amount was absorbed through the surface fluid conducting to the generation of vapor, whilst the underneath fluid was still subcooled. The authors concluded that the efficiency of the photothermal conversion process and the steam generation were enhanced almost linearly with increasing concentration of nanoparticles. Also, it was confirmed that an energy efficiency enhancement of nearly 95% using a gold nanofluid at 0.04% wt. in comparison with that attained with the water alone. Moreover, the researchers Du and Tang [27] numerically investigated the optical properties of plasmonic gold nanofluids with diverse morphologies, aspect ratios, and concentrations of the nanoparticles. The included gold nanostructures had the shape of nanoellipsoids, nanorods, and nanosheets. The obtained results indicated that the absorption peak of the gold nanoellipsoids and

gold nanorods could be increased by adjusting the aspect ratio. The size of the nanoparticles had only little impact on the extinction coefficient. Because of the plasmon resonance absorption band in the near-infrared and visible spectra, the plasmonic nanoparticles containing nanofluids possessed an improved performance in the solar energy storage even at very low concentrations and small sizes, which attains an improved stability. Regarding this, the authors proposed the gold blended nanofluids composed of 20% nanoellipsoids with two of aspect ratio, 60% nanorods having five of aspect ratio, and 20% nanosheets with l/h equal to seven, in view of the plasmon resonance absorption band. With these gold blended nanofluids it was attained an enhancement in the solar energy storage of 104% as compared to that achieved with gold spherical nanoparticles at very low concentrations and small sizes, which somewhat prevents the lack of stability of the nanofluids at high concentrations. **Figure 1** schematically represents the gold nanofluids synthesis method based on the dissolution of citrate crystals and stirring. **Figure 2** summarizes the fundamental benefits of the gold nanoparticles. **Figure 3** schematically illustrates a one-step method and a two step-method to prepare gold nanofluids.

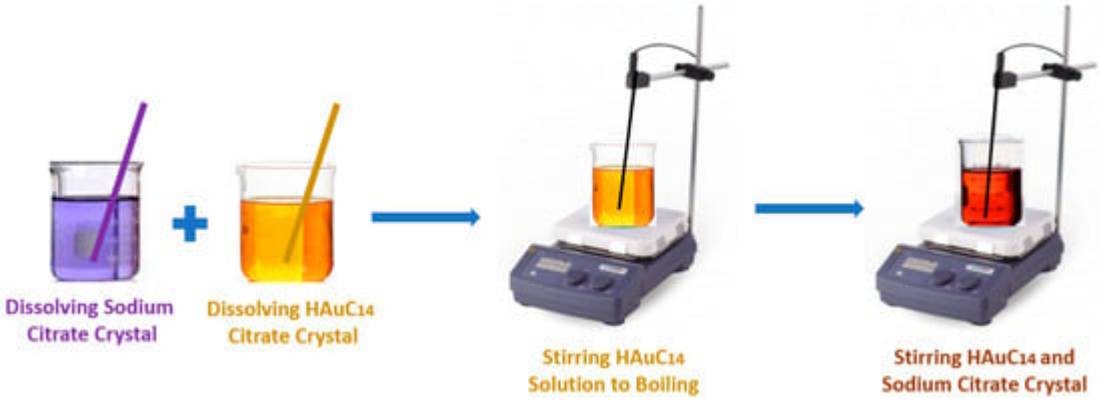

Figure 1. Gold nanofluids synthesis method based on citrate crystal dissolution.

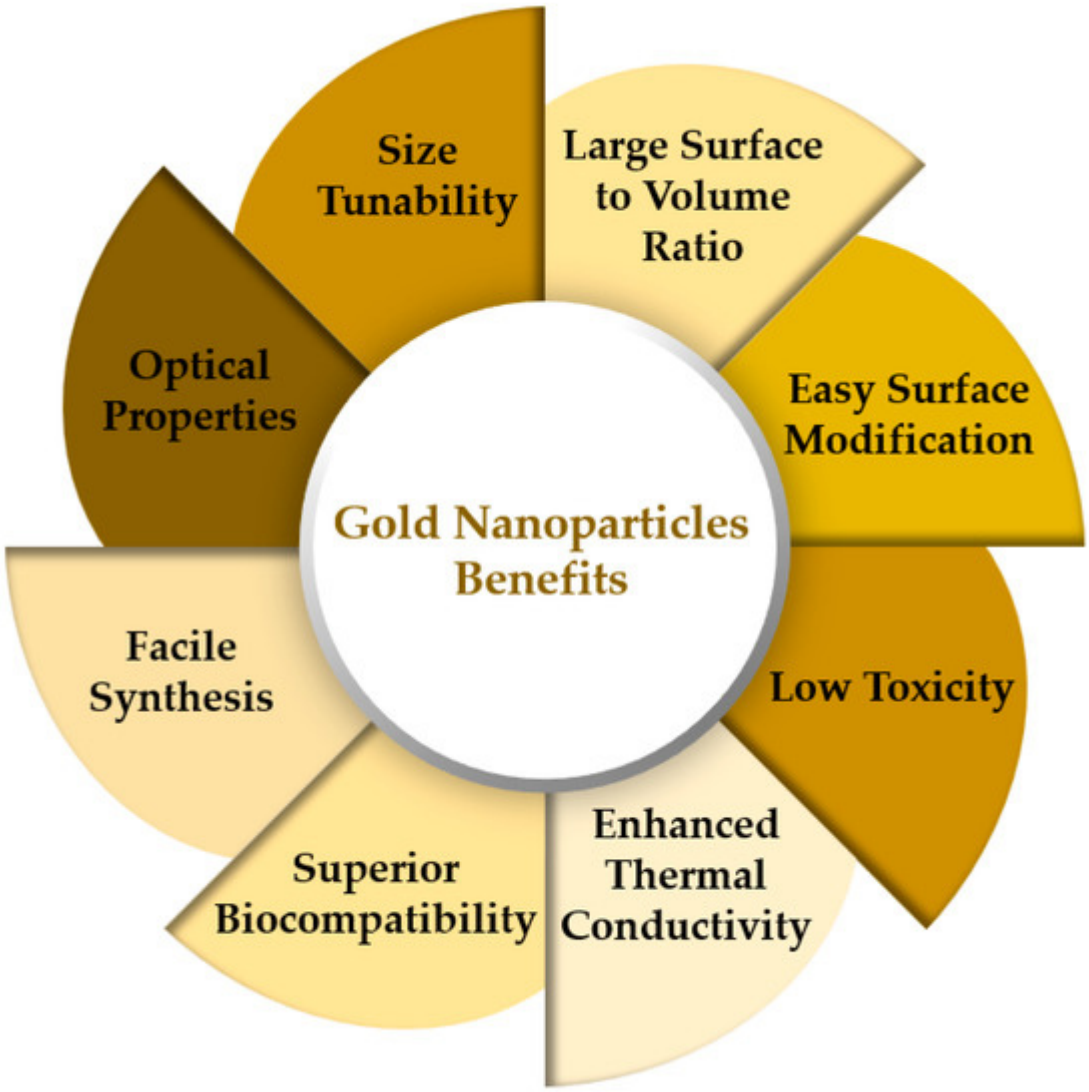

Figure 2. Main benefits of the gold nanoparticles.

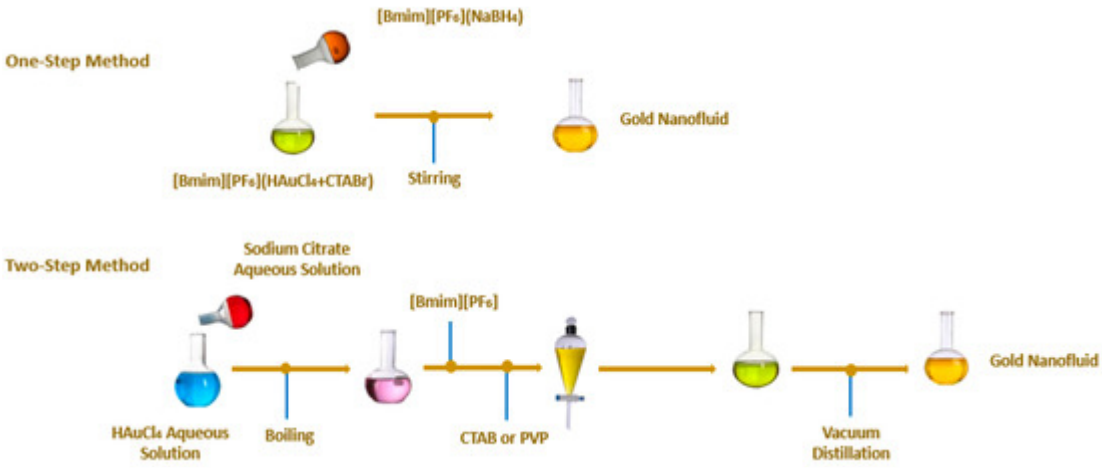

Figure 3. Typical one-step method and two step-method to produce gold nanofluids.

Table 1 summarizes the main findings of published experimental and numerical works on the gold nanofluids.

Table 1. Main findings on the gold nanofluids.

Authors	Morphology of the Nanoparticles	Concentration of the Nanoparticles	Base Fluid	Main Findings	Observations	Reference
Shalkevich et al.	Spherical with 2 to 45 nm	0.00025% vol.–1% vol.	Water	TC increase of 1.4% at 0.11% vol. and 40 nm	Addition of EGMUDE surfactant	[28]
Kim et al.	Near-Spherical with 7.1 to 12.1 nm	0.018% vol.	Water	TC increase of 9.3%	Stable after one month without any surfactant	[29]
Abdelhalim et al.	Spherical with 10/20 nm Hexagonal with 50 nm	0.01% vol.	Water	The larger nanoparticles with 50 nm exhibited higher viscosity than the smaller ones with 10 nm and 20 nm	The electrical conductivity increased with increasing size of the nanoparticles	[30]
Chen and Wen	Spherical and Plate-Shaped with 10 to 300 nm	764 μM/L	Water	TC increase of around 65%	The ultrasonication is a very powerful tool in engineering particle size and shape The TC was dependent on the particle shape and size	[31]
Wang et al.	Spherical with 5.2 ± 1.2 nm	0.000255% vol., 0.00051% vol., and 0.00102% vol.	[Bmim]PF_6	TC increase of 13.1% vol.	Addition of CTABr surfactant	[32]
Lopez-Munoz et al.	Near-Spherical with 16 nm to 125 nm	0.2 mg/mL to 1 mg/ml	Water	TD increase of 4.5% at 1 mg/mL with 55 nm	The TD ratio increased with increasing concentration	[33]
Torres-Mendieta et	Spherical with 20 nm to	---	Therminol VP-1 and	TC increase of around	Addition of PBS surfactant	[34]

Authors	Morphology of the Nanoparticles	Concentration of the Nanoparticles	Base Fluid	Main Findings	Observations	Reference
al.	nearly 750 nm		TOAB	4.1%		
John et al.	Spherical, Star-shaped and Bean-shaped	0.26 nM to 2.31 nM	Water	TD depended on the shape and concentration of the nanoparticles	The TD values indicate an enhancement in the TC and a decrease in the SH	[35]
Zeiny et al.	Spherical with 2.5 nm to 9 nm	30 mg/L to 150 mg/L	Water	Photothermal conversion increase of around 72%	The specific absorption rate of the gold nanofluids was superior to that of copper nanofluids	[36]
Yuan et al.	Spheres, Triangles, and Rods		Ketone, alcohol, ACN, THF	Ketone and alcohol formed gold nano-scaled spheres ACN and THF formed rods and triangles	The gold triangles and rods had more tendency to aggregate	[37]
Nimmagadda et al.	Spherical with 50 nm and 70 nm	2% vol.	Water	The nanofluid at 2 vol.% with 50 nm caused an increase in the convective heat transfer efficiency around 13%	The convective heat transfer efficiency increased with increasing Reynolds number and it was optimal in the magnetic field located along the X-axis	[38]
Zaaroura et al.	Spherical with 2.2 nm, 5 nm, and 10 nm	1% vol.	Water	The uncapped nanofluids with PBS solution showed that the nanoparticle	Addition of citrate-capping PBS and no citrate-PBS	[39]

Authors	Morphology of the Nanoparticles	Concentration of the Nanoparticles	Base Fluid	Main Findings	Observations	Reference
				size of 5 nm caused the greatest increase in the evaporation rate of 35% than the ones with 10 nm The citrate-capped nanofluids showed opposite results, the larger nanoparticles of 10 nm had the greatest increase in the evaporation rate of 15% but still less than the solution with PBS only		
Chen et al.	Sphere and rod with 20 nm	0 ppm to 200 ppm	Water	The solar absorption efficiency of the dimer nanofluid was enhanced by 21.2% when compared with the blended nanofluid with the same number of sphere and rod	Utilization of a thin layer of a plasmonic dimer nanofluid composed of a sphere and rod in water	[40]
Fogaça et al.	Spherical with 14 ± 2 nm	Two concentrations around 10^{-5}% vol.	Water	The less concentrated nanofluids were more	Use of a shell and helically coiled tube heat	[41]

3.2. Silver Nanofluids

Authors	Morphology of the Nanoparticles	Concentration of the Nanoparticles	Base Fluid	Main Findings	Observations	Reference
				efficient, suggesting the presence of a range of gold concentration for improving the heat transfer	exchanger with flowrates of 20 l/h, 30 l/h, and 40 l/h	
[44]						
Han et al.	Spherical with 20 nm, 40 nm, 60 nm, and 80 nm [46]	1 ppm to 80 ppm	Water and Ethylene Glycol	The optimal Merit Function of 1.95 and exergy efficiency of around 14% was achieved filtered by gold + PVP/ethylene glycol nanofluid at 29.2 ppm and 2 mL/min.	[45] Addition of PVP or PEG	[25]

les in the et al. [42] nductivity s of silver et al. [43] fractions possess fulfill the or human logy and nductivity t transfer research ce for the ation with maximum et al. [47] found an to that of the water itself under the same conditions. Consequently, the nanofluids showed better heat transfer capability as compared to water in common heat pipes since the nanoparticles can flatten the temperature difference of the fluids and decrease the boiling limit. Additionally, the authors Khamliche et al. [48] produced silver nanofluids in ethylene glycol and reported a 23% increase in the thermal conductivity when the nanofluids were aged for five hours. Also, silver nanoparticles in ethanol at 1% vol. and with polyvinylpyrrolidone as stabilizer [49] resulted in silver nanoparticles with shorter size that caused low viscosity, Newtonian behavior, and considerably higher thermal conductivity. Nonetheless, silver nanoparticles dispersed in diethylene glycol at nearly 4.4% vol. exhibited Newtonian behavior at high viscosity [50]. However, distinct literature findings have showed that the silver nanofluids exhibit non-Newtonian behavior, especially under low shear rates. The influencing factors of this behavior may include the concentration of nanoparticles, shear rate range, and dynamic viscosity of the base fluid. Furthermore, there exists a growing interest from the research community for silver nanostructures since they offer enhanced thermophysical characteristics [51]. The silver nanoparticles have already been synthesized through the evaporation-condensation technique. Nonetheless, this technique possesses some limitations and technical difficulties since the employed tube furnace occupies a lot of space, requires high amounts of energy for increasing the temperature around the source nanomaterial, and it needs prolonged periods to obtain thermal stability. Also, the chemical reduction is the most employed methodology to produce silver nanoparticles in the bottom-up route [52]. In this sense, diverse inorganic and organic reducing agents in different solutions are employed for the silver ions reduction. Examples of often added reducing agents are the polyethylene glycol copolymers, sodium citrate, sodium borohydride, and N,N-dimethyl formamide [53]. Moreover, some capping agents are also employed for the stabilization of the size of the nanoparticles. The most prominent benefit of this method is the capability of

synthesizing a considerable yield of nanoparticles in a short period. However, this method entails the use of toxic chemicals and results in toxic by-products. Hence, an alternative way to produce silver nanoparticles is the biosynthesis, which does not require toxic chemicals and it is complete environmental benevolent process for producing nanomaterials. The green synthesis of silver nanoparticles uses as precursor and reducing agents plant extracts, plant biomass and microorganisms. Also, this type of syntheses is cost-effective, scalable, not energy demanding, and do not require high temperature values and hazardous chemical products [53]. Furthermore, the researchers Nyamgoudar et al. [54] manufactured silver nanoparticles and nanorods through chemical reduction to produce and evaluate the resulting nanofluids. The authors reported that both silver nanoparticles and nanorods exhibited a thermal conductivity peak at a volumetric concentration of 2% vol. The silver nanorods nanofluids showed better results in comparison to those attained with the nanoparticles. The corresponding enhancement peaks were nearly 53% at 313 K for the nanoparticles and of around 78% at 323 K for the nanorods. Also, it was confirmed that the thermal conductivity decreased with increasing concentration of silver nanoparticles or nanorods because of the nanoparticle clustering that occurred at higher concentrations. The thermal conductivity of the nanofluids was also found to increase with increasing temperature values. Moreover, the researchers Hasan and Sultan [55] evaluated the thermal performance of a V-basin tube solar collector with 20 nm-sized silver nanoparticles dispersed in ethylene glycol and distilled water at volumetric fractions between 1% vol. and 5% vol. The nanofluids provided an appreciable performance enhancement of the V–basin tube solar collector translated in a higher heat transfer capability and thermal conductivity as compared to that of the ethylene glycol and distilled water. The silver nanofluids obtained an improvement when it was compared to the distilled water and ethylene glycol mostly at a increased inlet temperature values. The authors concluded that the size of the nanoparticles was of relevance in the heat transfer enhancement and thermal performance of the solar collector. It should be emphasized that the authors also did a comparative analysis with nanofluids having titanium oxide nanoparticles. The researchers concluded that the silver nanofluids provided extra enhancements in the thermal solar parameters in respect to those attained with the titanium oxide nanofluids. Also, the solar collector efficiency for the silver nanofluids was larger than the one achieved when using titanium oxide nanofluids due to the smaller silver nanoparticles and corresponding higher thermal conductivity. It was also reported that the difference between the inlet and outlet temperature of the silver nanofluids was increased due to the heat rate of the solar collector and lossless heat in the cases where the concentration of the nanoparticles was increased. Additionally, the researchers Seyhan et al. [56] inferred the effect of silver nanoparticles stabilized with surfactants on the thermal conductivity of hexane, ethylene glycol, and water. The silver nanoparticles were prepared in aqueous medium using the gum arabic surfactant and oleic acid/oleylamine to the silver nanoparticles stabilization. There were achieved up to 10% enhancements in the thermal conductivity of the ethylene glycol and hexane at 2% wt. and 1% wt. of silver nanoparticles, respectively. Nonetheless, it was confirmed that a nearly 10% decrease in the effective thermal conductivity employing the 1% wt. silver aqueous nanofluids. The silver nanoparticles performed quite better in ethylene glycol in which the stabilizer did not reduce the base fluid thermal conductivity. At a temperature of 20 °C, the inclusion of silver nanoparticles into the hexane provided enhancements of 3% and 11% at 0.06% vol. and 0.13% vol., respectively. Also, an enhancement of nearly 10% was observed for the ethylene glycol nanofluid at 0.11% vol. The increase in the effective thermal conductivity was attributed to the thermal diffusion and Brownian motion of the nanoparticles. The thermal conductivity increase could be obtained by augmenting the concentration

of the nanoparticles. Nonetheless, the thermal conductivity increasing rate weakens at higher concentrations of the nanoparticles because of the eventual nanoparticle agglomeration. When the gum arabic was solubilized in ethylene glycol, it did not change the base fluid thermal conductivity. Nonetheless, when the gum arabic was solubilized in water it considerably reduced the water thermal conductivity. The deterioration of the thermal conductivity with the gum arabic coated silver nanoparticles was attributed to the stabilizer that reduced the water base fluid thermal conductivity. After the incorporation of low concentrations of silver nanoparticles, the evolution with temperature of the water remained unchanged. Nonetheless, above a concentration threshold of nanoparticles, the nanofluids temperature dependency was altered. This reversal effect in the temperature dependency was explained by the authors based on the hydrogen bonding inhibition among the water molecules because of the gum arabic presence that furnished alternative hydrogen bonding sites. Moreover, the authors Zhang et al. [57] prepared silver nanowires by polyvinylpyrrolidone with a molecular weight of 40,000 and reported that the thermal conductivity enhancement of the nanofluids incorporating silver nanowires could be as high as nearly 13% at only 0.5% vol. of concentration, in reference to that obtained with the base fluid alone. The thermal conductivity value was nearly 0.28 W/mK, which was greater than the one attained with spherical silver nanoparticles of approximately 0.26 W/mK. The research team concluded that the molecular weight of the polyvinylpyrrolidone had impacted considerably on the final morphology of the silver nanowires and on the thermal conductivity of the corresponding nanofluids. The researchers used the model of Hamilton-Crosser to fit their experimental results and found that these were consistent with the ones provided by the model. Also, the authors Iyahraja and Rajadurai [58] produced nanofluids by dispersing polyvinylpyrrolidone coated silver nanoparticles in distilled water. It was measured the thermal conductivity of the nanofluids through the transient hot wire method and the obtained results demonstrated that the thermal conductivity of the nanofluids augmented with decreasing size of nanoparticles and increasing concentration of nanoparticles. It was verified a thermal conductivity increase of 54% in comparison with the one obtained with the distilled water alone at a low volumetric concentration of 0.1% vol. of 20 nm-sized silver nanoparticles. The researchers also reported that the surfactant and operating temperature had an appreciable influenced on the increase of the thermal conductivity of the nanofluids. The nanofluid temperature enhancement from 30 °C to 60 °C provided a 60% enhancement in the thermal conductivity, whilst the inclusion of surfactants decreased the thermal conductivity enhancement to only 34% using the polyvinylpyrrolidone and to only 31.5% using the sodium dodecyl sulfate. Additionally, the researchers Parametthanuwat et al. [59] experimentally studied the thermal performance of 0.5% wt. aqueous silver nanofluids at temperature values between 20 °C and 80 °C and potassium oleate and oleic acid as surfactants at concentrations from 0.5% wt. to 1.5% wt. The researchers found that the nanofluids at 1% wt. of potassium oleate yielded the best thermal performance improvement of approximately 28% at a temperature of 80 °C in reference to that of the water itself. Moreover, the nanofluid containing potassium oleate exhibited a higher thermal conductivity and specific heat dynamic than those attained with the water alone. The shear stress of the nanofluid increased with increasing shear rate from 101 s^{-1} to 103 s^{-1}. For a given concentration value of surfactant, the shear stress and dynamic viscosity of the base fluid decreased with increasing working temperature, confirming that the temperature directly influenced the viscosity and shear stress of the nanofluids. The thermal conductivity of the nanofluid with the surfactant increased with increasing operating temperature. The surfactant had contributed directly to the specific heat increase. Also, the authors verified that the oleic acid group surfactant contact angles

had better wettability characteristics, depending on the content of surfactant. Besides, the 1% wt. potassium oleate containing nanofluid could be quite effective for diminishing the wettability. The oleic acid group improved the stability of the nanofluids. It could be concluded that the nanofluids with surfactant provided a greater thermal performance improvement over the nanofluids without surfactant by nearly 80%. In sum, the oleic acid contributed clearly to the heat transfer rate increase of the silver nanofluids. Also, the improvement of the properties of the fluid with the potassium oleate conducted to the amelioration of the thermal characteristics and, consequently, offered better features than the ones provided by the inclusion of oleic acid. The ideal concentration for the addition of oleic acid and potassium oleate in the working fluid was of 1% wt. Furthermore, the researchers Asmat-Campos et al. [60] considered a prototype of solar heating systems by thermosiphon assisted by a halogen light presenting wavelengths between deep infrared and violet. The green synthesis of the silver nanoparticles explored the precursor and reducer silver nitrate of the alcoholic extract from wine production residues, obtaining spherical colloids having sizes between 30 nm and 40 nm. The obtained results of the application to solar thermal systems with radiant floor heating systems demonstrated that the silver aqueous nanofluid and silver oil nanofluid had an improved radiant heat transport and emission, being the best case the one of the silver oil nanofluid with a temperature increase rate of 0.6 °C/5 min and considering the temperature difference in the fluid attained a rate of nearly 2.6 °C/5 min and a specific heat capacity of 3519.4 J/kg °C. **Figure 4** schematically represents a green synthesis method to produce silver nanofluids.

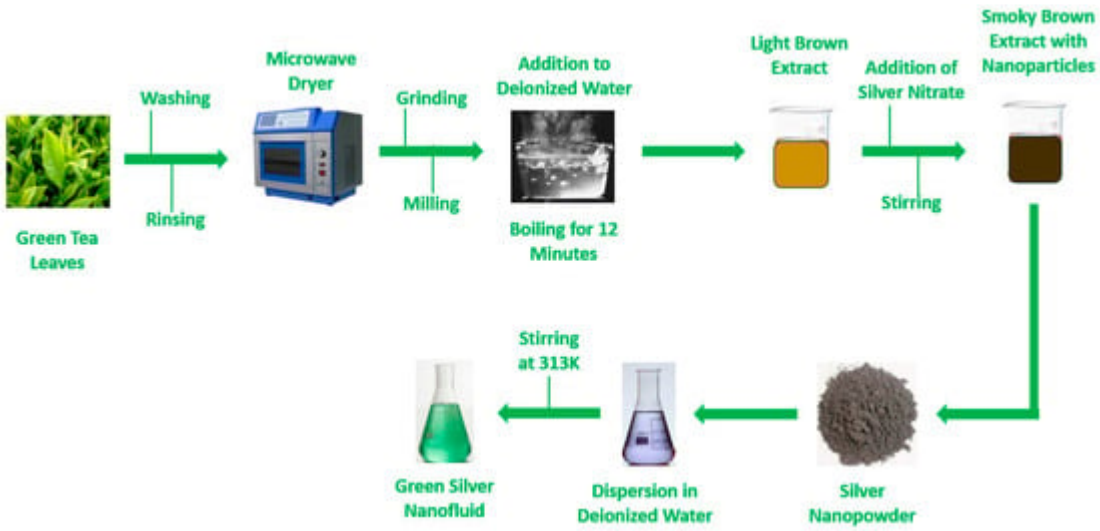

Figure 4. Bio-friendly synthesis methods to prepare silver nanofluids. Adapted from [61].

Figure 5 schematically represents a green synthesis method to produce silver nanofluids from wine grape pomace.

Figure 5. Green synthesis method to produce silver nanofluids from wine grape residues. Adapted from [60].

Figure 6 schematically represents the thermal conductivity increases in reference to that of water of silver nanoparticles and nanorods.

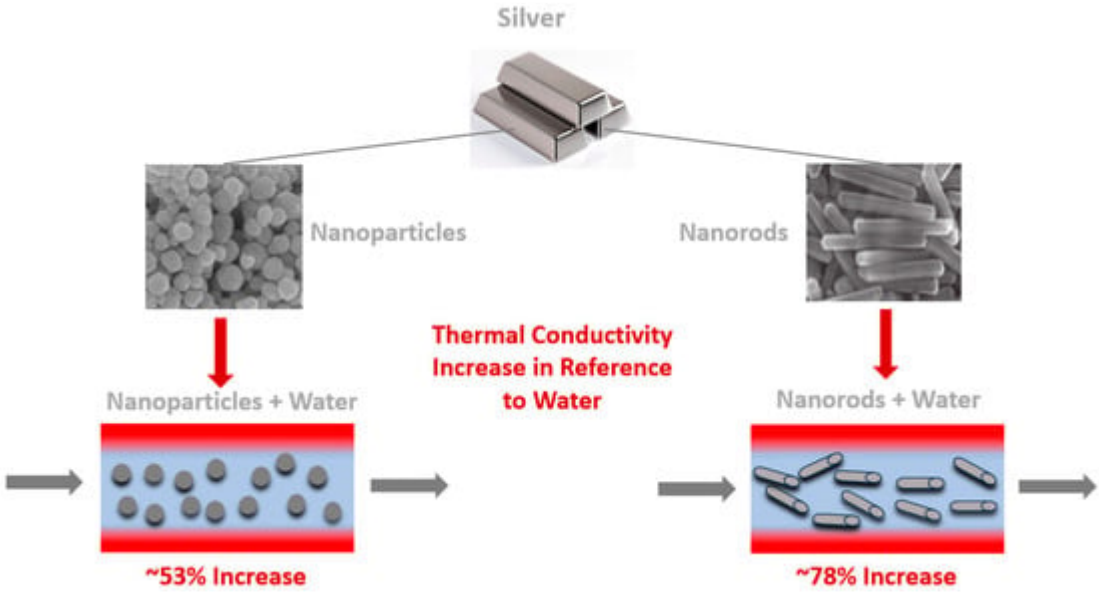

Figure 6. Heat transfer capabilities of silver nanoparticles and nanorods. Adapted from [54].

Table 2 presents the main findings of published experimental and numerical works on the silver nanofluids.

Table 2. Main findings on the silver nanofluids.

Authors	Morphology of the Nanoparticles	Concentration of the Nanoparticles	Base Fluid	Main Findings	Observations	Reference
Singh and Raikar	Spherical with 30 nm to 60 nm	1% vol.	Ethanol	1.55-fold increase in the TC	Addition of PVP	[49]
Kathiravan et al.	Spherical with 15 nm	0.25% wt., 0.5% wt., and 0.75% wt.	Water	TC was 2.5 times greater at a heat flux of 250 kW/m^2 at 0.75% wt.	Addition of sodium lauryl sulfate	[62]
Moreira et al.	Spherical with 15.17 nm	0.000426	Water	15.9% increase in the TD	The smaller nanoparticles gave a better enhancement in the heat transfer	[63]

Authors	Morphology of the Nanoparticles	Concentration of the Nanoparticles	Base Fluid	Main Findings	Observations	Reference
Madah et al.	Spherical with 40 nm	0.25% vol. to 5% vol.	Water	The TC increased linearly with increasing concentration of nanoparticles	The electrical conductivity increased considerably with increasing concentration of nanoparticles	[64]
Salehi et al.	Spherical with 3 nm to 11 nm	0 ppm to 1000 ppm	Water	Maximum increase in the TC of nearly 18%	Addition of PVP	[6]
Sarafraz et al.	Spherical with 50 nm	0.5% wt., 1% wt., and 1.5% wt.	Coconut Oil	Increase in the TC of 60% at 1.5% wt.	The TC slightly increased and the viscosity decreased with increasing temperature The TC and viscosity increased with increasing concentration of nanoparticles	[65]
Zhu et al.	Nanowires with 100 nm of diameter and 20 µm and 100 µm of length	5 mg·mL^{-1} to 20 mg·mL^{-1}	Ethylene Glycol	At 20 mg·mL^{-1} the photothermal conversion efficiency of the 20 µm and 100 µm nanowires were of 43.3% and 46.1%, respectively	The 100 µm long silver nanowires nanofluid had a higher photothermal conversion efficiency than the 20 µm ones	[51]
Zeroual et al.	Spherical with 2–3 nm	---	Ethylene Glycol	Increase in the TC of 2.5–3%	Addition of various contents of	[66]

Authors	Morphology of the Nanoparticles	Concentration of the Nanoparticles	Base Fluid	Main Findings	Observations	Reference
					latex copolymer	
Walshe et al.	Spherical with 5 nm to 110 nm	---	Water	Enhancements of 5–32% in the photo-thermal conversion efficiency	Addition of PVA	[67]
Oliveira et al.	Spherical with 10 nm and 80 nm	0.1% vol.–0.3% vol.	Water	The maximum increase in the TC was 18% at 0.3% vol.	Little increase in the viscosity at 0.3% vol.	[46]
Nakhjavani et al.	Spherical with 25 nm, 45–50 nm, and 75 nm	0.1% wt.–0.4% wt.	Water	Increase in the TC of approximately 45%	Optimal concentration of 0.1% wt.	[61]
Contreras et al.	Spherical	0.01% vol., 0.05% vol. and 0.1% vol.	Water/Ethylene Glycol 50:50	Increase of up to 4.4% in the heat transfer rate	The pumping power at high temperatures and mass flow rates increased by up to 4.1%	[68]
Selvam et al.	Spherical with diameters up to 100 nm	0.05% vol., 0.1% vol. and 0.15% vol.	Water/Ethylene Glycol 70:30	The maximum enhancement of TC was around 12% at 0.15% vol. and 50 °C	The SH decreased with increasing concentration and increased with increasing temperature Maximum decrease in the SH of around 7% at 0.15% vol. and 40 °C	[69]
Seifikar et al.	Spherical with 4.5 nm	0.002 g/100 mL, 0.005 g/100 mL,	Polyethylene Glycol	The surface temperature reached	Highly Stable Nanofluids	[1]

[70]

based on spherical platinum nanoparticles were capped by hydrophobic hyperbranched polyglycerol (HPG) with 1.2 nm and enhanced dispersion ability in hydrocarbons were fabricated employing an easy phase transfer procedure. The nanofluids of methylcyclohexane and platinum nanoparticles presented a remarkable stability after six months of storage. In a

Authors	Morphology of the Nanoparticles	Concentration of the Nanoparticles	Base Fluid	Main Findings Observations	Reference
		and 0.008 g/100 mL		around 52 °C with a ΔT of 24 °C under 1 Sun solar simulator light intensity for 1 h	

e energy
xchanger
o thermal
Pt-HPG-
9.6% wt.
nperature
kg having

an enhancement of nearly 21% in respect to the thermal cracking 1.98 MJ/kg. To gain the 2.2 MJ/kg heat sink, the 675 °C point could be reduced to 664 °C, 653 °C, and 638 °C for methylcyclohexane and Pt-HPG-MW = 3000, Pt-HPG-MW = 5000, and Pt-HPG-MW = 13,000, respectively. The increases in the heat sink and cracking were attributed to the catalysis of the platinum nanoparticles. Moreover, the researchers Wu et al. [71] fabricated platinum-hydrocarbon nanofluids initiated and stabilized with a hyperbranched polymer for thermal management purposes in advanced hypersonic aircraft. The hydrocarbon-dispersible platinum nanoparticles capped with modified hyperbranched polyethyleneimine having an average size of 2.4 nm were prepared by the phase transfer method. The stability over time of the nanofluids produced from the methylcyclohexane was affected by the alkyl chains length, and the methylcyclohexane and platinum-hyperbranched polyethyleneimine-C16 presented the highest stability. With the nanofluids at 0.005% wt., the dynamic viscosity was reduced by 2% in comparison to methylcyclohexane and the density remain unchanged. The batch reactor cracking of the nanofluids had considerable advantages as compared to the thermal cracking, which was contributed by the catalytic dehydrogenation of the platinum nanoparticles and the hyperbranched polyethyleneimine initiation effect, which was increased by the platinum nanoparticles. The tubular reactor supercritical cracking experiments mimicking the cooling channel of hypersonic aircraft revealed an ameliorated behavior of the nanofluids through conversion, gas yield, and heat exchangers. At a temperature of 650 °C, the conversion of methylcyclohexane raised from 12.4% wt. to 33% wt., the heat exchanger capability augmented from 1.99 MJ/kg to 2.24 MJ/kg, and the gas yield increased from 0.36 mmol/g to 4.01 mmol/g at a concentration of 0.006% wt. of platinum nanoparticles. To obtain the 2.1 MJ/kg heat exchanger performance, the temperature could be decreased from 664 °C to 642 °C. The liquid and gaseous products analyses of gaseous confirmed that the reactions forming unsaturated hydrocarbons with greater enthalpies and hydrogen were the favorites for the nanofluids cracking. Besides, the JP-10 (jet propellant) cracking application and platinum-hyperbranched polyethyleneimine also showed an enhanced performance. Hence, the authors concluded that platinum-hydrocarbon nanofluids having a hyperbranched polymer acting as stabilizer and initiator are very promising fuels with enhanced cracking performance and are very suitable to be applied in the thermal management in advanced hypersonic aircraft.

3.4. Palladium Nanofluids

Figure 7 presents the main methodologies to produce palladium nanoparticles.

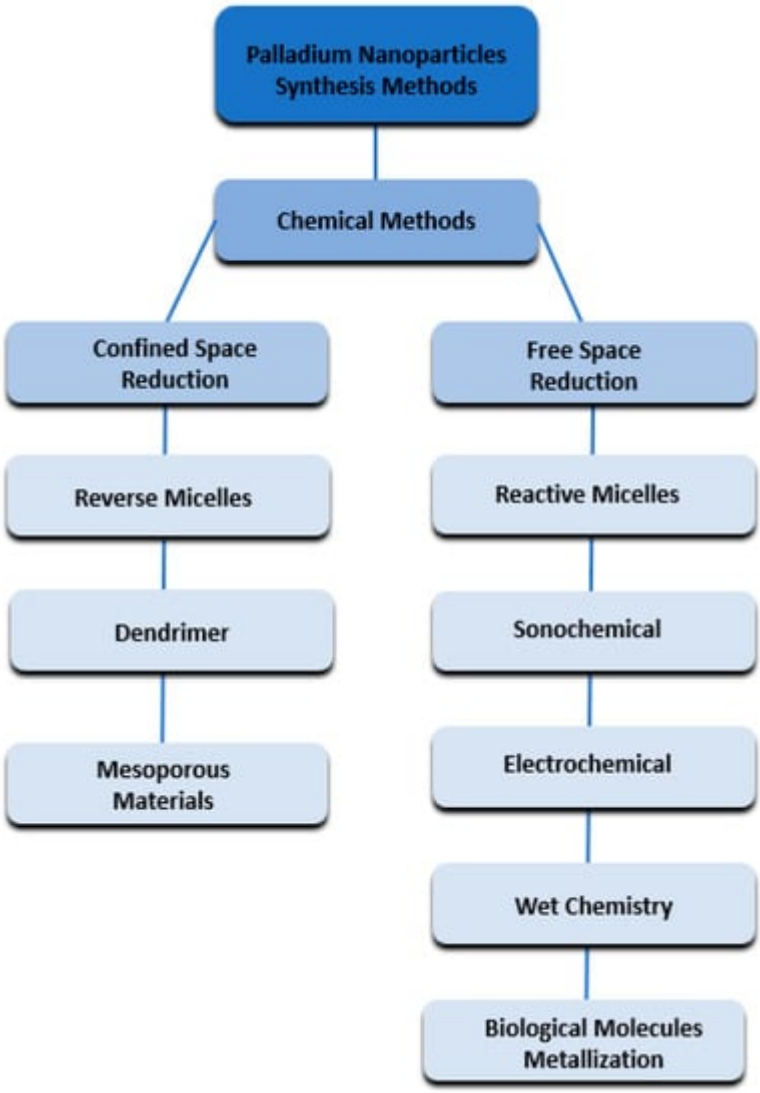

Figure 7. Fundamental methods to produce palladium nanoparticles.

The authors Carrilo-Berdugo et al. [24] prepared and characterized palladium nanoplates dispersed in oil nanofluids and evaluated their adequacy to be used as heat transfer fluids and volumetric absorbers for concentrated solar power systems. Concentrations in the order of 0.02% vol. of these nanomaterials promoted the spectral extinction of the visible spectrum, suggesting that these palladium nanofluids were very promising choices for volumetric absorption purposes. The same nanomaterial content was enough to cause a 11.5% thermal conductivity enhancement with palladium nanoplates at 100 °C and to enhance the specific heat by 12.9% with palladium nanoplates at 250 °C, with no increases in the dynamic viscosity, which suggested that the developed nanofluids are also very suitable alternatives for heat transfer enhancement purposes. Besides, the authors reported that the palladium nanoplate nanofluid could improve the efficiency of a volumetric parabolic-trough collector for concentrated solar power stations by around 32%. Also, the nanofluid could reduce the pumping power demand by 15%, minimized the structural alterations, and ensured the structural integrity of the collectors by preventing their overheating. Moreover, the researchers Carrilo-Berdugo et al. [72] discussed how the modification magnitude of the specific heat and thermal conductivity of the base fluid depended on the surface chemistry of the dispersed nanomaterials. The authors found that at 0.01% wt. of palladium nanoplates dispersed in a diphenyl oxide and

biphenyl eutectic mixture, the specific heat capacity was increased by around 12.5%, and the thermal conductivity was increased by 6% at 373 K. The researchers confirmed through density functional theory and molecular dynamics simulations that the molecules of the base fluid were chemisorbed on the palladium surfaces. The authors proposed that the stronger interactions at solid–liquid interfaces, the greater the specific heat enhancements, and the lower the thermal conductivity enhancements at high temperature values. Besides, the researchers Carrilo-Berdugo [73] elaborated an in-depth examination of the heat transfer and optical characteristics of palladium aromatic oil nanofluids, presenting promising results as heat transfer fluids and volumetric absorbers in the parabolic trough concentrated solar power stations. The authors found that at 0.03% wt. of concentration, the palladium nanoplates increased by 90% the sunlight extinction after a propagation length of 20 nm. The thermal conductivity was enhanced by 23.5% at a temperature of 373 K that was sufficient to increase the efficiency of the system by up to 45.3% and to decrease the pumping needs by 20%, with minimum collector length increases. The molecules chemisorbed at the interface acted as shelter boundaries that inhibited the heat transport, behaving as thermal resistance enhanced pathways, which strongly reduces the effects of the solid on the viscosity, given that it weakens the interactions between the nanoplates and the non-adsorbed molecules of the base fluid. The sunlight extinction was of 53%, 90% and 98% after 20 nm of propagation and at 0.006% wt., 0.03% wt., and 0.060% wt., suggesting that the palladium nanofluids are very suitable to be applied as volumetric absorbers. Furthermore, the effective thermal conductivity augmented by 2.6%, 11%, 17% and 23.5% at 0.03% wt. and at temperature values of 298 K, 323 K, 348 K, and 373 K. The viscosity, in the studied range of temperature values and concentrations, remained practically the same. Moreover, the researchers noted that in reference to the surface parabolic-trough collector using the common Dowtherm TMA thermal fluid, the volumetric absorption with the palladium nanofluids enhanced the efficiency of the system by 45% and, simultaneously, reduced the pumping power demand by 20%. Also, the length increase of the solar collector was minimum when using the palladium nanofluids turning the system much more cost-effective. Additionally, the molecular dynamics analysis demonstrated the effects of the palladium nanoplates on the momentum and heat transfer capabilities of the nanofluids. The momentum transfer can be quantified by the dynamic viscosity and the heat transfer by the thermal conductivity and were sensitive to the adsorption mode of the molecules of the base fluid on the solid-liquid interface. Hence, the solid-liquid interface interactions could become a novel route to further enhance the thermophysical characteristics of the nanofluids and stimulates the evaluation of what solid-liquid pairs should be candidates for the heat transfer and volumetric absorption in the concentrating solar power plants. Furthermore, the researchers Qin et al. [74] prepared palladium nanoparticles with modified hyperbranched polyglycerol stabilizers with good dispersion in non-polar organic solvents producing nanofluids with enhanced stability. The nanoparticles were synthesized with hyperbranched polyglycerol products modified with cyclohexanethiol, dodecanethiol, and octadecanethiol, which are herein named Pd-C, Pd-D, and Pd-O to simplify their identification. The thermal conductivity and stability improvements of the Pd-C, Pd-D, and Pd-O nanoparticles nanofluids were studied at various temperatures. The diameters of the nanoparticles stabilized using cyclohexanethiol, dodecanethiol, and octadecanethiol were between 2.7 nm and 3.6 nm. Also, the palladium nanoparticles can be dispersed uniformly in nonpolar base fluids like decalin. The Pd-D and Pd-O nanoparticles containing nanofluids remained stable at room temperature for 330 days. The nanofluids thermal conductivity increased with augmenting concentration of the nanoparticles and working temperature in comparison to that of the base fluid. The long alkyl chain modified hyperbranched polyglycerol mitigated the

agglomeration of the nanoparticles and aided the improvement of the thermal conductivity of the nanofluids. Besides, the thermal stability of the nanofluids decreased with rising temperature. Also, it was found that the palladium nanofluids thermal conductivity augmented with rising operating temperature and concentration of the incorporated nanoparticles. In general, the palladium nanoparticles stabilized by long-chain alkyl-modified hyperbranched polyglycerol exhibited superior thermal conductivity and stability over time than the ones that were not stabilized with the polyglycerol. Moreover, the authors Carrilo-Berdugo et al. [73] examined the specific heat of nanofluids with palladium nanoplates dispersed in a diphenyl oxide and biphenyl azeotropic eutectic mixture for concentrated solar power purposes. The developed nanofluids were stable for two weeks after the preparation and their density increased by 0.1%. The researchers observed that the specific heat of the nanofluids at concentrations of 0.012% wt., 0.03% wt., and 0.006% wt., increased by approximately 6%, 7%, and 5% at 100 °C, respectively, and nearly 14%, 17%, and 10% at 200 °C, respectively. Also, the authors observed that the evolution in function of the operating temperature was linear having the slope diverging in reference to the base fluid. Hence, it was concluded that the palladium nanoplates increased the sensible heat storage with increasing working temperature. Also, the palladium nanofluids were considered by the researchers as representative for the interfacial molecular layering analysis. Using density functional theory simulations, it was determined that both biphenyl and diphenyl oxide molecules chemisorbed evenly on palladium (111) and (100) plan surfaces. Hence, the formation of a high-temperature stable molecular layer on the solid–liquid interface was possible. This layer was expected to affect the thermophysical properties of the nanofluids. Additionally, the authors Cruz et al. [75] studied the possibility of using palladium nanofluids in the hyperthermia therapy. The authors highlighted that the palladium nanoparticles can be explored for hyperthermia therapy to increase the localized absorption of energy by external sources, to eliminate tumor cells be only heating them and with only little thermal damages imposed on the adjacent healthy cells. The palladium nanoparticles can also play the role of drug carriers acting on the tumor when heated to provide a localized antioxidant action and decrease cancer cells viability. Consequently, the palladium hydride nanoparticles can be adopted as promising materials for hyperthermia therapeutic processes. The $PdCeO_2$ nanoparticles and palladium nanocubes were synthesized and the nanofluids prepared with them were hydrogenated. The nanofluid having palladium nanocubes showed significant temperature increases of more than 30 °C after 3 min of diode-laser irradiation. Also, the nanofluids having $PdCeO_2H$ nanoparticles showed temperature increases of approximately 11 °C under similar irradiation conditions. The behavior of the $PdCeO_2H$ nanofluids was because of the ion H^+ in reducing the ion Ce^{4+} to Ce^{3+}. The palladium nanocubes were produced through chemical precipitation with the addition of the CTAB surfactant. The mechanical grinding and internal oxidation were also employed to fabricate a nanostructured $PdCeO_2$ alloy that displayed the formation of nano-scaled ceria in the palladium matrix. The temperature changes verified in the nanofluids were much greater than those verified with the distilled water alone, demonstrating the superior photothermal performance of the employed nanoparticles, including those that were hydrogenated. Moreover, the authors Yue et al. [76] investigated diverse palladium nanoparticles modified by octadecanethiol, octadecylamine, and a mixture of them were prepared, which are named herein by Pd-S, Pd-N, and Pd-S+N, respectively. The size of the palladium nanoparticles was from 1 nm to 3 nm and they were well-dispersed in kerosene. The researchers verified that the Pd-S+N was the most promising additive for the hydrocarbon fuel for preparing a highly stable propellant, thermal conductivity, and cooling ability. The investigation team found that the viscosity of the nanofluids containing palladium nanoparticles

with concentrations inferior to 0.2% wt. had no appreciable increase in respect to the viscosity of the kerosene. Besides, the researchers reported that the thermal conductivities of the nanofluids were considerably enhanced at 0.2% wt. of palladium nanoparticles. The stability trend of the nanofluids were as follows: Pd-S+N > Pd-S > Pd-N. The pyrolysis of decalin in the absence/presence of palladium nanoparticles was carried out from 440 °C to 470 °C. The order of the catalytic ability for the palladium nanoparticles was as follows: Pd-N > Pd-S+N > Pd-S. The catalytic activities of the surface-modified nanoparticles for pyrolysis of decalin were attributed to the synergistic effects of palladium and its ligands. Hence, it was concluded that the functional nanoparticles could be synthesized by adjusting the relative content of the core palladium and its ligands in the nanoparticles. The researchers verified that the Pd-S+N was the most promising additive for the hydrocarbon fuel for preparing a highly stable propellant, thermal conductivity, and cooling ability. **Figure 8** schematically illustrates a typical green synthesis method for palladium nanoparticles obtained from the *Origanum vulgare* plant.

Figure 8. Typical green preparation method to synthesize palladium nanoparticles from *Origanum vulgare* plant.

3.5. Ruthenium Nanofluids

In the last decade, novel pairs of anions and cations based on water and ionic liquids were evaluated for green energy technology enhancement processes to substitute the conventional salt solutions to avoid the problems of corrosion, sedimentation in addition to working temperature limitations. It was already confirmed that the solid nanoparticles of metals and metal oxides present greater thermal conductivities than those of the traditionally employed fluids by order of magnitude. The Ionanofluids can be employed as novel heat transfer fluids and media for the improvement of green energy applications. Most of the previous study focuses on loading nanoparticles in ionic liquids to study their thermophysical characteristics like viscosity, thermal conductivity, and density, which have emerged as new generation heat transfer fluids. Ionic liquids provide a flexible liquid platform to prepare and stabilize transition metal nanoparticles. By synthesizing nanoparticles directly in ionic liquids enhances the stability of nanofluids. The authors Patil et al. [77] developed the in-situ production of ruthenium nanoparticles in imidazolium based ionic liquid with cation 1-butyl 3-methyl imidazolium and various anions chloride, bromide, iodide, and tetrafluoroborate. After the preparation ruthenium nano dispersion characterized with UV-Visible for absorption

study, HR-TEM for morphology and X-ray photoelectron spectroscopy for electronic structural analysis, ATR-IR spectroscopy for structural analysis. Properties like the thermal conductivity, dynamic viscosity, and density of the nanofluids were determined to evaluate the heat transfer applicability of the ruthenium nanofluids. The researchers focused on the influence of the anion on the size of the ruthenium nanoparticles and their effect on thermophysical properties like density, viscosity, and thermal conductivity. As an anion changes thermophysical properties varied with the respective anion.

3.6. Iridium, Osmium, and Rhodium Nanofluids

The authors Bonet et al. [78] synthesized iridium nanoparticles having a narrow size distribution through the chemical reduction of the metal species in ethylene glycol. The average size of the nanoparticles was reported to be inferior to 10 nm for all the cases. The size of the nanoparticles was adjusted fundamentally by altering the initial metal concentration, temperature of reaction, and concentration of the employed polyvinylpyrrolidone in the process. The iridium nanoparticles were produced by dissolving at room temperature an amount of polyvinylpyrrolidone in 75 mL ethylene glycol under magnetic stirring. After that it was added the metal compound. After the solid dissolution, the solution was heated at a rate of 1 °C/min until a pre-defined temperature value. The reaction was maintained at constant temperature for a period. Then, a regulated heating mantle was employed to perform the synthesis of the metal under a fixed heating rate and at constant temperature. The iridium nanoparticles prepared at 100 °C without polyvinylpyrrolidone were free of sintering. The iridium nanoparticles average size was found to be about 3 nm. The iridium nanoparticles after the preparation stage and dispersed in ethylene glycol compose a as prepared nanofluid. These nanofluids, together with the ones composed of iridium nanoparticles dispersed in water, and mono alcohols should be in-depth studied. Particularly, for testing their capability in heat transfer processes, given that their ability to work as catalysts in chemical reactions has already been proved. The hybrid forms of iridium-ruthenium are also promising. Moreover, the authors Zhang et al. [79] reported a simple one-pot solvothermal synthesis of from to 1.5 nm to 2.5 nm-sized monodispersed iridium nanoparticles, porous nanodendrites, and worm-like chain nanowires for which the carbon monoxide oxidation reaction was explored as probe reaction to infer the impact of the size of the nanoparticles and surface-capping materials on the catalytic ability. The authors noted that the main contributor for the production of nanodendrites and nanowires was the attachment mechanism through strong adsorption of the halide anions Br^- and I^- on the facets of the nanoclusters of or by diminishing the iridium precursors reduction rate by changing their concentrations during preparation. Also, the annealing tests revealed that a treatment under O_2-H_2 atmosphere was an effective way to remove the iridium nanoparticles surface-capping organics supported on commercially available silica. The catalytic carbon monoxide oxidation reaction showed that a considerable increase in the catalytic activity of the carbon monoxide oxidation reaction was attained along with the activation energies alteration after the treatment for the catalysts of the iridium nanoparticles. It should be emphasized that the catalytic activity increase might be due to the surface modifications such as the removal of the surface capping organics, amount of iridium species in metallic and oxidized states, and different number of active sites for the nanocatalysts during the specific atmospheric treatment. Once again, it should be noted that the different synthesized forms of iridium nanostructures should be dispersed in adequate base fluids and applied in heat

transfer performance experimental works. Furthermore, there are rather scarce published works on the preparation of osmium [80] and rhodium nanoparticles [81].

3.7. Bimetallic Nanofluids

The bimetallic nanoparticles composed of two different metals have attracted considerable attention due to their unique properties relevant for several applications including catalysis, sensing, optics, electronic devices, and medicine [82]. The bimetallic nanoparticles have also been applied to design bio sensors, to fabricate targeted drug delivery carriers and to increase the luminescence of the nanoparticles. The bimetallic nanoparticles of copper have also received much attention because of their novel properties and applications [83]. For instance, the copper-palladium nanoparticles have been prepared by several methods and because of many potential applications [84]. These studies confirm that copper-palladium bimetallic nanoparticles are easy to fabricate and relatively cheaper catalysts. The preparation and characterization of the metallic nanoparticles with diverse configurations, thermophysical properties, sizes and shapes have been the focus of the research community in the field. Also, considerable emphasis has been given to the production of colloidal bimetallic nanoparticles because of their improved optical, magnetic, electric, and catalytic properties over those of the single metallic nanoparticles. The bimetallic counterparts can be applied in a broad range of purposes including catalysts, sensors, biomedical imaging, drug delivery, and quantum dots [84]. The inclusion of a second metal alters the physicochemical properties of the individual constituents and offers synergistic-driven features derived from the interactions between the components [85]. As an example, the researchers Singh et al. [86] evaluated the catalytic activity of nickel-palladium nanoparticles. The research team observed a high hydrogen selectivity of more than 80% for the decomposition of hydrous hydrazine at 50 °C. The corresponding monometallic counterparts were either have poor activity like the nickel nanoparticles or were inactive including the palladium nanoparticles. Moreover, the authors Feng et al. [87] verified an appreciably higher catalytic activity when gold-platinum nano-sized dendrites were used in the methanol oxidation in respect to that of the commercially available catalyst of platinum-carbon. The authors interpreted the result based on the enhanced electronic interaction among the constituents of the nanoparticles. Furthermore, the researchers Kumari et al. [88] synthesized gold-silver bimetallic nanoparticles with pomegranate fruit juice and observed an increased catalytic activity and nitric oxide and hydroxyl radical scavenging activity with the developed nanoparticles. Besides, the pairing of gold and platinum was already frequently explored by the researchers. The gold nanoparticles possess an large application spectrum due to the inherent wide absorption band over the visible region in, for instance, plasmonic photothermal therapies, photovoltaics, therapeutic agents, and electronic conductors [89]. A feature of great relevance of the gold nanoparticles is the adjustable optoelectronic ability that can be tuned according to the morphology and agglomeration degree of the nanoparticles [90]. The platinum nanoparticles exhibit enhanced antioxidation and catalytic characteristics usually employed in the petrochemical cracking and electrocatalytic processes [91]. The platinum nanoparticles due to inherent favorable Fermi level positioning and superior electron interactions are very suitable to be applied in the hydrogen evolution and oxygen reduction reactions as electrocatalysts. Nonetheless, the bimetallic gold-platinum nanoparticles have shown superior performance in different purposes as compared to either of their constituents. Also, the authors Ledendecker et al. [92] reported the preparation of gold-platinum core–shell nanorods for catalytic and medical applications. Moreover, the authors Lucas et al. [93] reported the formation of hollow gold-platinum and gold-

palladium nanoparticles through galvanic replacement reactions. Additionally, the authors Wang et al. [94] deposited gold and platinum bimetallic nanostructures on palladium nanocubes for oxidizing the glucose. The authors reported that in transient catalysis, the gold-palladium nanocubes showed a wide linear range between 0.25 mM and 14 mM and great sensitivity of around 13.6 $\mu A \cdot mM^{-1} \cdot cm^{-2}$ in determining the d-glucose in reference to the platinum-palladium nanocubes. The catalyst exhibited remarkable recoveries between 99.2% and 100.1% for sensing the d-glucose. Furthermore, the growth of platinum nanoparticles on gold nanoplates having enhanced photo response has also been published. Moreover, the researchers Lou et al. [95] synthesized platinum with triangular gold nanoprisms and proposed them for hydrogen generation. Besides, the researchers Zhang and Toshima [96] developed a simultaneous reduction method to fabricate gold-platinum nanoparticles having stable and improved catalytic activity in the oxidation of glucose. Given that the gold-platinum nanoparticles exhibit a third order nonlinear phenomenon because of the intense optical Kerr effect, they can be great contenders to produce gyroscopic systems. The ultrasonic non-destructive testing evaluates the materials during the processing and after the fabrication. Controlling the characteristics of the materials by monitoring the structural inhomogeneity, phase transition, thermal conductivity, size, and dislocations that will forecast the potential uses of the materials can be accomplished through measuring the frequency dependent ultrasonic absorption. In the last years, many researchers have studied the ultrasonic behavior of aqueous solutions to better understand the underlying mechanisms to attain an improved control over the procedure. It has been confirmed that in fluidic suspensions, the dispersants tend to diminish the wave propagation caused by weak particle-liquid interactions, whilst the nanoparticles increase the wave propagation because of the enhnecd nanoparticle-fluid interactions. **Figure 9** schematically represents a synthesis method for gold-platinum nanoparticles.

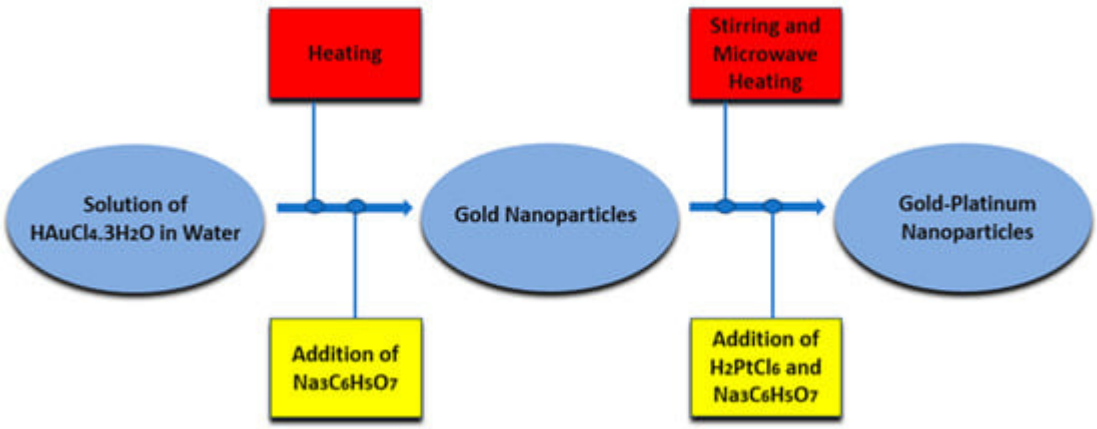

Figure 9. Synthesis method for gold-platinum nanoparticles. Adapted from [96].

The nanofluids can represent a case study for better understanding the governing mechanisms of the ultrasonic behavior in suspensions due to the great variety of possible manipulations that can be attained by the adjustment of their chemical composition and concentration. A reduced attenuating ability of the nanofluids might conduct to an improved performance in ultrasound imaging. The attenuation impacts also on the propagation of waves and signals in optical fibers, electrical circuits, and air, making such issue pivotal in the telecommunications field of actuation. Hence, there should be developed fluidic systems having increased wave propagation or mitigated attenuation for an improved performance. The water-based metallic nanofluids are themselves a special alternative

as they possess superior plasmonic characteristics [97] and ultrasound properties. Only a few research works were carried out on the ultrasonic features of the metallic nanofluids. In this sense, the authors Verma et al. [98] verified a frequency dependent ultrasonic attenuation in the water-based gold and gold-platinum nanofluids. The gold and gold-platinum nanofluids were synthesized by the microwave-assisted citrate reduction. The nanofluids were characterized through X-ray diffraction, revealing a distinct two-phase bimetallic crystal structure with no alloy formation, The nanofluids were also characterized by UV-vis spectroscopy that showed two plasmonic bands in the bimetallic species having a aggregation tendency. The high-resolution microscopy analysis revealed spherical nanoparticles having sizes from 15 nm to 30 nm presenting marked lattice spacings of platinum and gold. The bimetallic nanofluids demonstrated a lower resistance to ultrasonic waves in respect to that of the gold nanofluids. The thermal conductivity at distinct concentration values of both nanofluids had significant enhancements in reference to that of the water, although the gold-platinum platinum exhibited lower enhancements in respect to those of the gold nanofluids. Such fact was attributed to the mixed metallic structure in which the platinum with much poor thermal conductivity reduced the thermal conductivity of the bimetallic species. The lower thermal conductivity might explain the lower attenuation of the bimetallic nanofluids since it was already demonstrated that the thermal conductivity is proportional to the ultrasonic attenuation. The fact that gold-platinum bimetallic nanofluids could have lower attenuation because of the lower thermal conductivity in reference to that of the gold nanofluids may have appreciable repercussion in diverse fields of actuation like ultrasound imaging and optochemical sensors. **Figure 10** summarizes the fundamental preparation methods of the bimetallic nanoparticles.

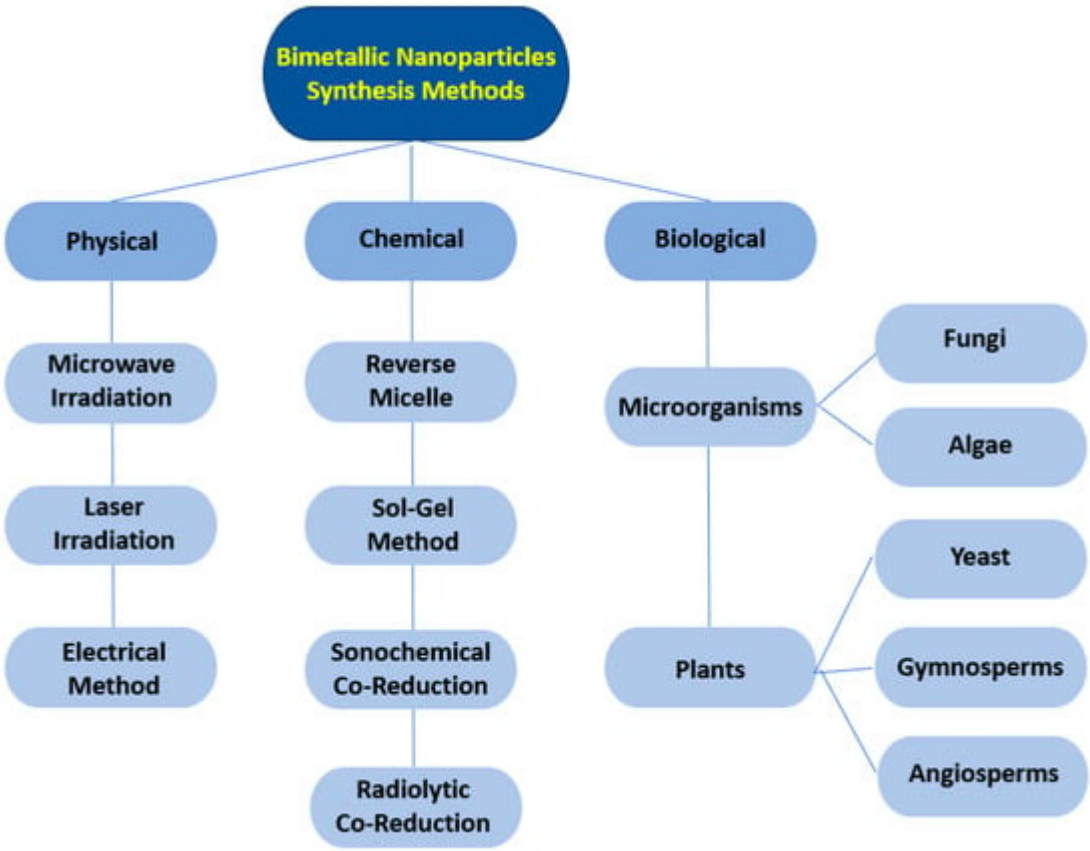

Figure 10. Fundamental preparation methods of the bimetallic nanoparticles.

Table 3 presents the main findings on the published works on the bimetallic nanofluids.

Table 3. Main findings on the bimetallic nanofluids.

Authors	Nanoparticles	Concentration of the Nanoparticles	Base Fluid	Main Findings	Observations	Reference
Chen et al.	Gold-Silver	0.00025% vol.	Water	Highest solar photothermal conversion efficiency of around 41.4%	The efficiency of the system using bimetallic nanoparticles was higher than that using only gold nanoparticles of around 37.8% with a 40% decrease in the gold consumption	[99]
Zhu et al.	Gold-Silver/nitrogen-doped graphitic polyhedrons	5% wt.	Ethylene Glycol	The photothermal conversion efficiency increased by up to approximatelly 74.4%	Considerable broadband absorption in the visible and near-infrared spectrum at lower concentration	[100]
Sanchéz-Ramirez et al.	Gold-Palladium with Au/Pd = 12/1, 5/1, 1/1, 1/5 molar ratios	---	Water	The maximum diffusivity was achieved for the nanoparticles with highest gold/palladium molar ratio	The TD was strongly dependent on the composition of the nanoparticles	[101]
Gutierres Fontes et al.	Gold-Silver with core-shell structure at Au/Ag = 3/1, 1/1, 1/3, and 1/6 molar ratios	---	Water	Linear increment of the TD when the silver shell thickness is increased	The TD was sensible to the type of the metallic nanoparticles structure The TD was modified by altering the composition of the nanoparticles	[102]

Authors	Nanoparticles	Concentration of the Nanoparticles	Base Fluid	Main Findings	Observations	Reference
Dsouza et al.	Gold-Silver spherical with 30 nm	0% vol. to 1.0% vol.	Water	Increase in the TC of 7% at 0.6% vol. and the viscosity has nearly attained 6%	The TC and viscosity increases with increasing concentration of nanoparticles	[103]
	Silver-Copper with 65 nm	0% vol. to 1.0% vol. [104]	Water	Increase in the TC of 8% at 1% vol. and increase in the viscosity of about 72% at the same concentration	The TC and viscosity increased with increasing concentration of nanoparticles	

es in a base fluid to dispense the homogenous phase that they designated by hybrid nanofluids. It has been demonstrated in several published investigation studies that the hybrid nanofluids present increased thermal conductivity in respect to the conventional single nanofluids. The incorporation of hybrid nanoparticles into the base fluid causes an appreciable thermal conductivity enhancement. Still, there are many limitations associated to the exploration of hybrid nanofluids in domestic and industrial applications that should be overcome. Several researchers studied the hybrid nanofluids flowing in different possible configurations of real practical heat transfer processes, but they are very small in number. Only a few scientific articles have been dedicated to the hybrid nanofluids development and implementation. Also, the authors Gamachu and Ibrahim [105] assessed the motion of a hybrid viscoelastic nanofluid over a disk by considering silver and alumina dispersed in carboxymethyl cellulose water. Additionally, the authors Hayat and Nadeem [106] published relevant findings for the rotating motion of a hybrid nanofluid copper oxide and silver nanoparticles. Also, the researchers Singh et al. [107] developed a thermally conductive, stable, and surfactant-free hybrid nanofluid composed of in-house produced nanoflakes of silver decorated functionalized reduced graphene oxide. The reduced graphene oxide and hybrid form were efficient photocatalysts for the water-soluble azo dye tartrazine degradation. The hybrid nanofluid was tested on a custom-made engine test rig and a fuel consumption reduction was observed from 15% to 17%. Other factors were also significantly increased, which indicated that the developed nanofluid was a promising option to be applied as nanocoolant. Since graphene and silver have the highest thermal conductivity among the carbon materials and metallic materials, respectively, it is reasonable to consider that a hybrid material including both could be a better solution. Nonetheless, the fundamental challenge associated with the development of such enhanced nanomaterials was to ameliorate the stability over time of the graphene and silver dispersions in water. To mitigate such limitation, the authors functionalized the graphene oxide using the 2,4-diaminohydroxylpyrimidine that significatively improved the stability of the silver nanoparticles decorated functionalized reduced graphene oxide. The dimensions of the silver nanoparticles decorated over the graphene were between 10 nm and larger silver lumps, adopting distinct preparation methodologies. The Raman spectroscopic characterization showed the SERS property of the produced nanomaterials and, consequently, these ones are very suitable to be applied in sensors. The SERS property increased with increasing size of the silver nanoparticles and there was a rapid increase when their size decreased

from 50 nm to 10 nm. The results showed that the hybrid nanomaterial having the smallest silver nanoparticles exhibited the peak thermal conductivity enhancement of 24% at 0.25% wt. The improved stability of the dispersion was due to the existing functionality over the graphene sheet that promoted the molecule-to-base fluid and molecule-to-molecule interactions. Besides, the authors Naderi et al. [108] prepared a polyvinylpyrrolidone coated silver nanofluid at volumetric concentrations between 250 ppm and 1000 ppm by a two-step method. The thermophysical properties of the nanofluids were analyzed regarding their exploration in photovoltaic/thermal solar collectors. According to the results, the polyvinylpyrrolidone coated silver nanofluids thermal conductivity improved the base fluid properties, making the thermal conductivity coefficient to grow up to 50% at certain temperature values and increased from 0.59 for base fluid to 1.01 W/mK by increasing the fraction to up to 1000 ppm. Thus, the polyvinylpyrrolidone coated silver nanofluid could be considered as a novel operating fluid to improve the thermal efficiency of the photovoltaic/thermal systems. Due to pressing need of implementing renewable energy processes in buildings and the notorious dependency of the photovoltaic/thermal collectors on the thermophysical characteristics of the working fluids, the critical features of the polyvinylpyrrolidone-coated silver nanofluid were experimentally studied. The authors concluded that the stability analysis of the nanofluids indicated that the zeta potential of the polyvinylpyrrolidone-coated silver nanofluids was around acceptable −42 mV. Because of the low concentrations of the nanofluids, their density and specific heat have intangible alterations in comparison to the base fluid. The nanofluids thermal conductivity was noticeably enhanced with enhancing concentration of the nanofluids and operating temperature. This was explained by the thermal conductivity of the polyvinylpyrrolidone-coated silver nanofluid, which was approximately two times superior to the one of deionized water at 55 °C. Also, the authors found that the concentration that provided a more improved performance of the photovoltaic/thermal collector was of 1000 ppm of polyvinylpyrrolidone coated silver nanofluid. The highest thermal conductivity coefficient was 1.01, which was attained at a temperature of 55 °C and at 1000 ppm imposing to a greater amount of heat being conducted from the photovoltaic module, by this way accessing higher efficiencies. Moreover, the researchers Mbambo et al. [109] reported the fabrication method and thermal conductivity of gold nanoparticles decorated graphene nanosheets based nanofluids. The graphene-gold nanostructures were synthesized trough a nanosecond pulsed Nd:YAG laser with 1064 nm of wavelength to ablate a target made of graphite followed by gold in ethylene glycol to produce a graphene-gold nanoparticles-ethylene glycol hybrid nanofluid. The characterization process of the graphene-gold nanoparticles-ethylene glycol hybrid nanofluid revealed a sheet-like structure of graphene decorated with crystalline gold nanoparticles having 6.3 mm of average diameter. On the other hand, the gold nanoparticles appeared to be smaller with the graphene, showing the benefits from ablating gold nanoparticles in graphene-ethylene glycol. The examination of the thermal conductivity at temperature values from 25 °C to 45 °C indicated that the graphene-gold nanoparticles-ethylene glycol hybrid nanofluid exhibited a 0.41 W/mK thermal conductivity superior to that of graphene dispersed in ethylene glycol of 0.35 W/mK and gold nanoparticles disperse in ethylene glycol of 0.39 W/mK nanofluids. The hybrid nanofluids thermal conductivity was also superior to that of the ethylene glycol itself of 0.33 W/mK. The graphene-gold nanoparticles-ethylene glycol nanofluid displayed a thermal conductivity enhancement of 26% at temperature values from 25 °C to 45 °C, which was superior to other previously published enhancements of ethylene glycol-based nanofluids. The increased thermal conductivity of the graphene-silver nanoparticles-ethylene glycol nanofluid derived from the combined effect between the gold nanoparticles and the graphene that possess enhanced thermal conductivity values.

Besides, the poor thermal conductivity of the base fluid was due to the enhanced dynamic viscosity of the EG38. The experimental results make the developed hybrid nanofluid very suitable for enhanced heat transfer enhancement processes. It was not reported the impact on the heat transfer enhancement of the concentration of the nanoparticles as they were synthesized inside the base fluid. Furthermore, the researchers Yarmand et al. [110] proposed an innovative method of synthesis for the decoration of platinum on functionalized graphene nanoplatelets. The graphene-platinum nanostructures were manufactured by a simple chemical reaction process that incorporated an acid treatment for the functionalization of the graphene nanoplatelets. The graphene–platinum hybrid nanofluids preparation method did not involve any addition of surfactants. The stability of the nanofluids was good with no significant sedimentation after 22 days of test. The thermal conductivity of the graphene nanoplatelets–platinum dispersed in distilled water showed an enhancement of nearly 18% at a temperature of 40 °C and at 0.1% wt. The researchers also stated that all the tested concentrations of the graphene-platinum aqueous nanofluids exhibited higher thermal conductivity than the one of the distilled water alone. Also, the authors Wang et al. [111] prepared gold-palladium nanoparticles decorated on nitrogen-doped carbon nanotubes by using a polyethylene imine reduction procedure. The polyethylene played the role of reducing and stabilizing agent, facilitating the nanoparticles nucleation and growth on the surface of the nitrogen-doped carbon nanotubes. All the synthesized nanofluids showed a broadband absorption ability over the near infrared and visible spectra. The gold-palladium-nitrogen-doped carbon nanotubes nanofluids absorbed more solar irradiation when compared with the palladium-nitrogen-doped carbon nanotubes or gold-nitrogen-doped carbon nanotubes nanofluid. The photothermal conversion efficiency of gold-palladium-nitrogen doped-carbon nanotubes nanofluids was approximately 62% as compared with around 53% and 57% for palladium-nitrogen doped-carbon nanotubes and gold-nitrogen doped-carbon nanotubes, respectively. Such enhancement derived mainly from the synergetic effects of the nitrogen doped-carbon nanotubes and gold-palladium nanoparticles. In essence, the gold-palladium nanoparticles have been decorated successfully on the nitrogen-doped carbon nanotubes surfaces using the polyethylene imine reduction method. Additionally, the researchers Jaiswal et al. [112] synthesized copper-palladium hybrid nanostructures nanofluids at varying molar ratio. The temperature dependent thermal conductivity of the nanofluids was measured through a hot disc thermal constant analyzer. The impact of the varying molar ratio in the copper/palladium was inferred by transmission electron microscopy imaging observation. Joint nanorods type morphology was observed in the copper-palladium nanofluids with a molar ratio of 1:20. When increasing the copper content at a copper-palladium molar ratio of 1:1, a hybrid nanorods and spherical nanoparticles morphology was observed, which was further changed to uniform spherical shaped structure in the copper-palladium at 20:1 molar ratio. The nanofluids thermal conductivity augmented with increasing temperature. The significant enhancements in thermal conductivity of the nanofluids were observed on the suspension of copper-palladium bimetallic nanoparticles at different higher temperatures. The thermal conductivity enhancement maximum of nearly 18.8% was found at 80 °C for copper-palladium at 20:1 molar ratio. On the other hand, the researchers Aberoumand and Jafarimoghaddam [113] elaborated an investigation work on the preparation, and thermal conductivity and dielectric strength determination of silver-tungsten oxide hybrid nanofluids with transformer oil as base fluid. The nanofluids were produced via the electrical explosion of wire one-step methodology. The zeta potential of the nanofluids was determined at 1% wt., 2% wt., and 4% wt. and it was measured their thermal conductivity at temperatures between 40 °C and 100 °C. The investigation team reported that the electrical

conductivity of the nanofluids diminished to 35 kV at 4% wt. Also, the authors observed a thermal conductivity enhancement of 41% at 4% wt. The dielectric strength of the hybrid nanofluids decreased in reference to that of the pure transformer oil and this fact was attributed to the electrical conductivity of the silver nanoparticles since the tungsten oxide counterparts have poor electrical conductivity. **Figure 11** schematically illustrates the preparation method of silver nanoparticles decorated graphene oxide nanoflakes based nanofluids. **Figure 12** represents the synthesis method of gold nanoparticles decorated graphene nanosheets based nanofluids.

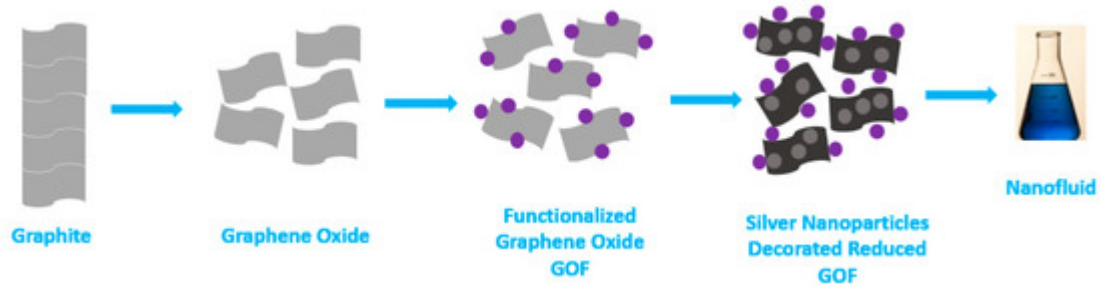

Figure 11. Synthesis method of silver nanoparticles decorated graphene oxide nanoflakes based nanofluids. Adapted from [107].

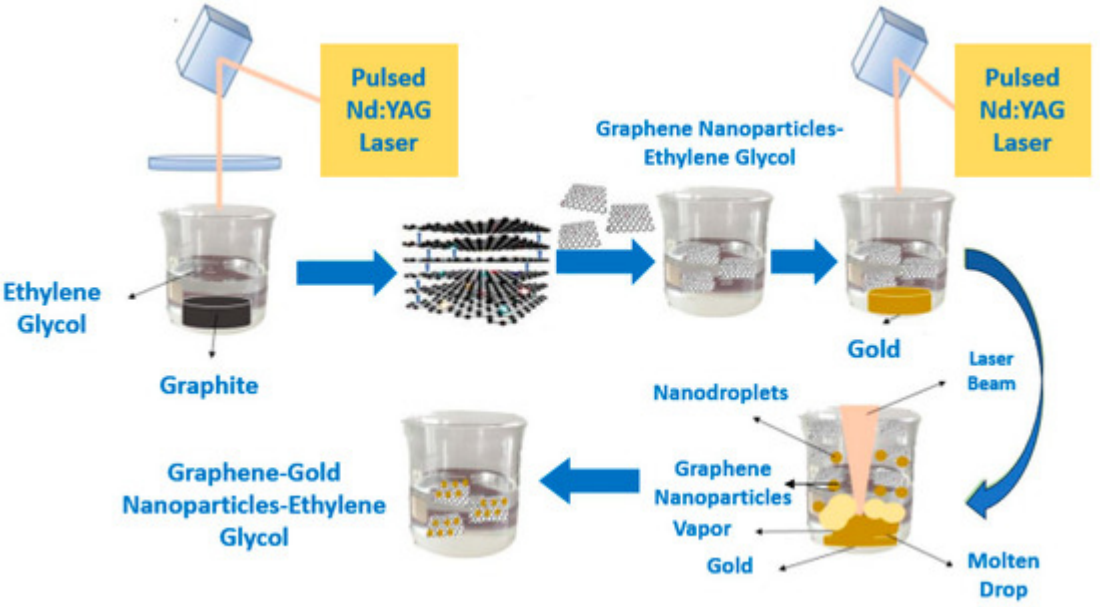

Figure 12. Synthesis method of gold nanoparticles decorated graphene nanosheets based nanofluids. Adapted from [109].

Table 4 presents the main findings of the experimental and numerical works on the noble metals hybrid nanofluids.

Table 4. Main findings on the noble metals hybrid nanofluids.

Authors	Nanoparticles	Concentration of the Nanoparticles	Base Fluid	Main Findings	Observations	Reference
Ma et al.	Silver-Graphene	0.001% wt., 0.002% wt., and 0.003 wt.	Water	Increase in the CHF of around 52.3% at 0.001% wt. Increase in the HTC of around 69.6% at 0.001% wt.	The bubble formation period of hybrid nanofluids was short and the bubble separation diameter was small	[114]
Li et al.	Silver-Titanium Oxide	100 ppm and 200 ppm	Water	200 ppm nanofluid produced ~1.4 times of the overall efficiency of the PV/T system compared to water. The merit function reached 2.16 at 100 ppm	The nanoparticles exhibited high absorptivity in the visible wavelengths and good transmittance in the spectral response range of the photovoltaic cell Tunable nanoparticle concentrations were adopted to obtain high-efficiency solar energy utilization	[115]
Hjerrild et al.	Core–shell silver-silica nanodiscs	0.026% wt.	Water	Increase in the efficiency by 30% of the PV/T collector by 30% at 0.026% wt.	The silver nanodiscs strongly absorb visible light with minimal scattering, whereas the silica shell maintains the shape and absorption	[116]

Authors	Nanoparticles	Concentration of the Nanoparticles	Base Fluid	Main Findings	Observations	Reference
					spectrum of the silver cores	
Munkhbayar et al.	Silver-Multi-walled carbon nanotubes with 100 nm (silver)	0.05% wt. MWCNTs–3% wt. silver	Water	Increase in the TC of 14%	Maximum absorbance of 2.506 abs at a wavelength of 264 nm	[117]
Baby and Ramaprabhu	Silver-Hydrogen Induced Exfoliated Graphene	0.05% vol.	Water	Increase in the TC of around 25%	The nanofluids were stable for three months	[118]
Chen et al.	Silver-Multi-walled carbon nanotubes	1% vol.	Water	Increase in the TC of around 24%	Higher TC than that of the MWCNTs nanofluids of around 12%	[119]
Botha et al.	Silver-Silica	0.6% wt. silver–1.4% wt. silica	Transformer Oil	The theoretical increase in the TC was lower than the experimental determined one, suggesting that there is a synergistic effect between the silver nanoparticles and silica Lower dielectric strength	Newtonian behavior at lower silica concentrations and Bingham flow at high concentrations Lower viscosity compared to the one of the silica nanofluids	[120]
Han and Rhi	Silver-Alumina	0.005% vol., 0.05% vol., and 0.1% vol.	Water	Made the heat pipe system deteriorate in terms of	Greater thermal resistance with increasing concentration	[121]

Authors	Nanoparticles	Concentration of the Nanoparticles	Base Fluid	Main Findings	Observations	Reference
				thermal resistance	of nanoparticles	
Dinarvand et al.	Gold-Zinc Oxide nanospheres and nanoplatelets	3.33% vol.	Water	Increase of 40% in the heat transfer rate	The heat transfer rate increases 2.2% more with the nanoplatelets than with the nanospheres	[122]
Jin et al.	Gold-Titanium Oxide spherical and oval with 12–15 nm	Gold 5 ppm and 10 ppm	Water	Increase of around 60.8% in the absorption efficiency	The light–to–heat conversion characteristics of hybrid nanofluids are not necessarily stronger than that of single nanofluids The ratio of different concentrations and the content of different components affected the results	[123]
Banianerian et al.	Gold-Titanium Oxide	0% vol. to 3% vol.	Water	Maximum increase in the latent heat of evaporation of around 27% at 0.1% vol. and 150 °C	Use of hybrid nanofluids to enhance the fluid LHE is rational just in high working pressures. (higher than 400 kPa) Increasing the concentration of nanoparticles at low pressures	[124]

s of Cu,
ability in

l activity
2021,

3. Xu, L.; Wang, Y.-Y.; Huang, J.; Chen, C.-Y.; Wang, Z.-X.; Xie, H. Silver nanoparticles: Synthesis, medical applications and biosafety. Theranostics 2020, 10, 8996–9031.

Authors	Nanoparticles	Concentration of the Nanoparticles	Base Fluid	Main Findings	Observations	Reference
					reduced the latent heat of evaporation, whereas at higher pressures the inverse trend was verified	

synthesized by a one-step method with the effect of polyvinylpyrrolidone on thermal behavior. Appl. Phys. Lett. 2013, 102, 231907.

7. Liu, D.; Chen, X.; Xu, G.; Guan, J.; Cao, Q.; Dong Bo Qi, Y.; Li, C.; Mu, X. Iridium nanoparticles supported on hierarchical porous N-doped carbon: An efficient water-tolerant catalyst for bio-alcohol condensation in water. Sci. Rep. 2016, 6, 21365.
8. Neumman, O.; Urban, A.S.; Day, J.; Lal, S.; Nordlander, P.; Halas, N.J. Solar Vapor Generation Enabled by Nanoparticles. ACS Nano 2013, 7, 42–49.
9. Otanicar, T.; Dale, J.; Orosz, M.; Brekke, N.; DeJarnette, D.; Tunkara, E.; Roberts, K.; Harikumar, P. Experimental evaluation of a prototype hybrid CPV/T system utilizing a nanoparticle fluid absorber at elevated temperatures. Appl. Energy 2018, 228, 1531–1539.
10. Gao, Y.; Yang, T.; Jin, J. Nanoparticle pollution and associated increasing potential risks on environment and human health: A case study of China. Environ. Sci. Pollut. Res. Int. 2015, 22, 19297–19306.
11. Elsaid, K.; Olabi, A.G.; Wilberforce, T.; Abdelkareem, M.A.; Sayed, E.T. Environmental impacts of nanofluids: A review. Sci. Total Environ. 2021, 763, 144202.
12. Du, J.Y.; Su, Q.M.; Li, L.; Wang, R.J.; Zhu, Z.F. Evaluation of the influence of aggregation morphology on thermal conductivity of nanofluid by a new MPCD-MD hybrid method. Int. Commun. Heat Mass Transf. 2021, 127, 105501.
13. Song, D.; Jing, D.; Ma, W.; Zhang, X. Effect of particle aggregation on thermal conductivity of nanofluids: Enhancement of phonon MFP. J. Appl. Phys. 2019, 125, 015103.
14. Wang, R.J.; Qian, S.; Zhang, Z.Q. Investigation of the aggregation morphology of nanoparticle on the thermal conductivity of nanofluid by molecular dynamics simulations. Int. J. Heat Mass Transf. 2018, 127, 1138–1146.
15. Wang, R.J.; Feng, C.; Zhang, Z.; Shao, C.; Du, J.Y. What quantity of charge on the nanoparticle can result in a hybrid morphology of the nanofluid and a higher thermal conductivity? Powder Technol. 2023, 422, 118443.

16. Jin, X.; Guan, H.Q.; Wang, R.J.; Huang, L.Z.; Shao, C. The most crucial factor on the thermal conductivity of metal-water nanofluids: Match degree of the phonon density of state. Powder Technol. 2022, 412, 117969.
17. Cui, X.; Wang, J.; Xia, G.D. Enhanced thermal conductivity of nanofluids by introducing Janus particles. Nanoscale 2021, 14, 99–107.
18. Guan, H.Q.; Su, Q.M.; Wang, R.J.; Huang, L.Z.; Shao, C.; Zhu, Z.F. Why can hybrid nanofluid improve thermal conductivity more? A molecular dynamics simulation. J. Mol. Liq. 2023, 372, 121178.
19. Zhang, H.; Chen, H.-J.; Du, X.; Wen, D. Photothermal conversion characteristics of gold nanoparticle dispersions. Sol. Energy 2014, 100, 141–147.
20. Sabir, R.; Ramzan, N.; Umer, A.; Muryan, H. An experimental study of forced convective heat transfer characteristic of gold water nanofluid in laminar flow. Sci. Int. (Lahore) 2015, 27, 235–241.
21. Chen, M.; He, Y.; Zhu, J.; Kim, D.R. Enhancement of photo-thermal conversion using gold nanofluids with different particle sizes. Energy Convers. Manag. 2016, 112, 21–30.
22. Burgos, J.; Mondragón, R.; Elcioglu, E.B.; Fabregat-Santiago, F.; Hernández, L. Experimental Characterization and Statistical Analysis of Water-Based Gold Nanofluids for Solar Applications: Optical Properties and Photothermal Conversion Efficiency. Sol. RRL 2022, 6, 2200104.
23. López-Munoz, G.A.; Balderas-López, J.A.; Ortega-Lopez, J.; Pescador-Rojas, J.A.; Salazar, J.S. Thermal diffusivity measurement for urchin-like gold nanofluids with different solvents, sizes and concentrations/shapes. Nanoscale Res. Lett. 2012, 7, 667. Available online: https://www.nanoscalereslett.com/content/7/1/667 (accessed on 12 July 2023.).
24. Carrilo-Berdugo, I.; Sampaio-Guzmán, J.; Dominguez-Nunez, A.; Aguilar, T.; Martinez-Merino, P.; Navas, J. Are Nanofluids Suitable for Volumetric Absorption in PTC-CSP Plants? An Exemplified, Realistic Assessment with Characterized Metal–Oil Nanofluids. Energy Fuels 2022, 36, 8413–8421.
25. Han, X.; Yao, Y.; Zhao, X.; Huang, J.; Khosa, A.A. Investigations of stable surface-modified gold nanofluids optical filters based on optical optimization for photovoltaic/thermal systems. Sustain. Energy Technol. Assess. 2023, 57, 103203.
26. Amjad, M.; Raza, G.; Xin, Y.; Pervaiz, S.; Xu, J.; Du, X.; Wen, D. Volumetric solar heating and steam generation via gold nanofluids. Appl. Energy 2017, 206, 393–400.
27. Du, M.; Tang, G.H. Plasmonic nanofluids based on gold nanorods/nanoellipsoids/nanosheets for solar energy harvesting. Sol. Energy 2016, 137, 393–400.

28. Shalkevich, N.; Escher, W.; Burgi, T.; Bruno, M.; Si-Ahmed, L.; Poulikakos, D. On the thermal conductivity of gold nanoparticle colloids. Langmuir 2009, 26, 663–670.
29. Kim, H.J.; Bang, I.C.; Onoe, J. Characteristic stability of bare Au-water nanofluids fabricated by pulsed laser ablation in liquids. Opt. Lasers Eng. 2009, 47, 532–538.
30. Abdelhalim, M.A.K.; Mady, M.M.; Ghannam, M.M. Rheological and dielectric properties of different gold nanoparticle sizes. Lipid Health Dis. 2011, 10, 208.
31. Chen, H.J.; Wen, D. Ultrasonic-aided fabrication of gold nanofluids. Nanoscale Res. Lett. 2011, 6, 198.
32. Wang, B.; Wang, X.; Lou, W.; Hao, J. Gold-ionic liquid nanofluids with preferably tribological properties and thermal conductivity. Nanoscale Res. Lett. 2011, 6, 259.
33. Lopez-Munoz, G.; Pescador-Rojas, J.; Ortega, J.; Santoyo, J.; Balderas-Lopez, J. Thermal diffusivity measurement of spherical gold nanofluids of different sizes/concentrations. Nanoscale Res. Lett 2012, 7, 423.
34. Torres-Mendieta, R.; Mondragón, R.; Juliá, E.; Mendoza-Yero, O.; Cordoncillo, E.; Lancis, J.; Mínguez-Vega, G. Fabrication of gold nanoparticles in Therminol VP-1 by laser ablation and fragmentation with fs pulses. Laser Phys. Lett. 2014, 11, 126001.
35. John, J.; Thomas, L.; Kurian, A.; George, S.D. Modulating fluorescence quantum yield of highly concentrated fluorescein using differently shaped green synthesized gold nanoparticles. J. Lumin. 2016, 172, 39–46.
36. Zeiny, A.; Jin, H.; Lin, G.; Song, P.; Wen, D. Solar evaporation via nanofluids: A comparative study. Renew. Energy 2018, 122, 443–454.
37. Yuan, M.; Li, Y.-B.; Guo, J.; Zhong, R.-B.; Wang, L.-P.; Zhang, F. Solvent effects on gold nanoparticle formation from pho-to-chemical reduction of Au(III) by UV irradiation. Nucl. Sci. Tech. 2018, 29, 158.
38. Nimmagadda, R.; Reuven, R.; Asirvatham, L.G.; Wongwises, S. Thermal Management of Electronic Devices Using Gold and Carbon Nanofluids in a Lid-Driven Square Cavity Under the Effect of Variety of Magnetic Fields. IEEE Trans. Compon. Packag. Manuf. Technol. 2020, 10, 1868–1878.
39. Zaaroura, I.; Harmand, S.; Carlier, J.; Toubal, M.; Fasquelle, A.; Nongaillard, B. Experimental studies on evaporation kinetics of gold nanofluid droplets: Influence of nanoparticle sizes and coating on thermal performance. Appl. Therm. Eng. 2021, 183, 116180.
40. Chen, Z.; Chen, M.; Yan, H.; Zhou, P.; Chen, X.-Y. Enhanced solar thermal conversion performance of plasmonic gold dimer nanofluids. Appl. Therm. Eng. 2020, 178, 115561.

41. Fogaça, M.B.; Dias, D.T.; Gómez, S.L.; Behainne, J.J.R.; Turchiello, R.F. Effectiveness of a Shell and Helically Coiled Tube Heat Exchanger Operated With Gold Nanofluids at Low Concentration: A Multi-Level Factorial Analysis. J. Thermal Sci. Eng. Appl. 2021, 13, 021029.
42. Sharma, P.; Baek, I.H.; Cho, T.; Park, S.; Lee, K.B. Enhancement of thermal conductivity of ethylene glycol based silver nanofluids. Powder Technol. 2011, 208, 7–19.
43. Warrier, P.; Teja, A. Effect of particle size on the thermal conductivity of nanofluids containing metallic nanoparticles. Nanoscale Res. Lett. 2011, 6, 247.
44. Ferdous, Z.; Nemmar, A. Health Impact of Silver Nanoparticles: A Review of the Biodistribution and Toxicity Following Various Routes of Exposure. Int. J. Mol. Sci. 2020, 21, 2375.
45. Pourhoseini, S.H.; Naghizadeh, N.; Hoseinzadeh, H. Effect of silver-water nanofluid on heat transfer performance of a plate heat exchanger: An experimental and theoretical study. Powder Technol. 2018, 332, 279–286.
46. Oliveira, G.A.; Filho, E.P.B.; Wen, D. Synthesis and characterization of silver/water nanofluids. High Temp. High Press. 2014, 43, 69–83.
47. Gupta, M.; Singh, V.; Kumar, S.; Dibaghi, N. Experimental analysis of heat transfer behavior of silver, MWCNT and hybrid (silver + MWCNT) nanofluids in a laminar tubular flow. J. Therm. Anal. Calorim. 2020, 142, 1545–1559.
48. Khamliche, T.; Khamlich, S.; Doyle, T.B.; Makinde, D.; Maaza, M. Thermal conductivity enhancement of nano-silver particles dispersed ethylene glycol based nanofluids. Mater. Res. Express 2018, 5, 035020.
49. Singh, A.K.; Raykar, V.S. Microwave synthesis of silver nanofluids with polyvinylpyrrolidone (PVP) and their transport properties. Colloid Polym. Sci. 2008, 286, 1667–1673.
50. Tamjid, E.; Gunther, B. Rheology and colloidal structure of silver nanoparticles dispersed in diethylene glycol. Powder Technol. 2010, 197, 49–53.
51. Zhu, D.; Huang, G.; Zhang, L.; He, Y.; Xie, H.; Yu, W. Silver Nanowires Contained Nanofluids with Enhanced Optical Absorption and Thermal Transportation Properties. Energy Environ. Mater. 2019, 2, 22–29.
52. Wang, H.; Qiao, X.; Chen, J.; Ding, S. Preparation of silver nanoparticles by chemical reduction method. Colloids Surf. A Physicochem. Eng. Asp. 2005, 256, 111–115.
53. Shameli, K.; Ahmad, M.B.; Jazayeri, S.D.; Sedaghat, S.; Shabanzadeh, P.; Jahangirian, H.; Mahdavi, M.; Abdollahi, Y. Synthesis and Characterization of Polyethylene Glycol Mediated Silver Nanoparticles by the Green Method. Int. J. Mol. Sci. 2012, 13, 6639–6650.
54. Nyamgoudar, S.M.; Silaparasetti, V.P.; Shilpa, M.P.; Pavithra, K.S.; Mundinamani, S.; Eshwarappa, K.M.; Surabhi, S.; Raman, K.; Ravikanara Ganesha, A.; Gurumurthy, S.C. Analysis

of shape dependency of thermal conductivity of silver-based nanofluids. J. Therm. Anal. Calorim. 2022, 147, 14031–14038.

55. Hasan, I.A.; Sultan, K.F. Performance Evaluation of the V–basin Tube Solar Collector by using different Nanoparticles and Base Fluids. Eng. Technol. J. 2018, 36, 461–470.
56. Seyhan, M.; Altan, C.L.; Gurten, B.; Bucak, S. The effect of functionalized silver nanoparticles over the thermal conductivity of base fluids. AIP Adv. 2017, 7, 045101.
57. Zhang, L.; Yu, W.; Zhu, D.; Xie, H.; Huang, G. Enhanced Thermal Conductivity for Nanofluids Containing Silver Nanowires with Different Shapes. J. Nanomater. 2017, 2017, 5802016.
58. Iyahraja, S.; Rajadurai, J.S. Stability of aqueous nanofluids containing PVP-coated silver nanoparticles. Arab. J. Sci. Eng. 2016, 41, 653–660.
59. Parametthanuwat, T.; Bhuwakietkumjohn, N.; Rittidech, S.; Ding, Y. Experimental investigation on thermal properties of silver nanofluids. Int. J. Heat Fluid Flow 2015, 56, 80–90.
60. Asmat-Campos, D.; Avalos, V.; Delgado, A.; Gutierrez, H.; Jacinto, P.; Reyes, Z. Synthesis and characterization of nanofluids from the biosynthesis of nanoparticles and their evaluation in solar thermal systems. E3S Web Conf. 2020, 167, 05003.
61. Nakjavani, M.; Nikkah, V.; Sarafraz, M.M.; Shoja, S.; Sarafraz, M. Green synthesis of silver nanoparticles using green tea leaves: Experimental study on the morphological, rheological and antibacterial behavior. Heat Mass Transf. 2017, 53, 3201–3209.
62. Kathiravan, R.; Kumar, R.; Gupta, A.; Chandra, R. Preparation and Pool Boiling Charcatreistics of Silver Nanofluids Over a Flat Plate Heater. Heat Transf. Eng. 2012, 33, 69–78.
63. Moreira, L.M.; Carvalho, E.A.; Bell, M.J.; Anjos, V.; Sant'Ana, A.C.; Alves, A.P.; Fragneaud, B.; Sena, L.Á.; Archanjo, B.S.; Achete, C.A. Thermo-optical properties of silver and gold nanofluids. J. Therm. Anal. Calorim. 2013, 114, 557–564.
64. Maddah, H.; Rezazadeh, M.; Maghsoudi, M.; Nasirikokhdan, S. The effect of silver and aluminum oxide nanoparticles on thermophysical properties of nanofluids. J. Nanostruct. Chem. 2013, 3, 28.
65. Sarafraz, M.M.; Arya, A.; Nikkhah, V.; Hormozi, F. Thermal Performance and Viscosity of Biologically Produced Silver/Coconut Oil Nanofluids. Chem. Biochem. Eng. Q. 2016, 30, 489–500.
66. Zeroual, S.; Estellé, P.; Cabaleiro, D.; Vigolo, B.; Emo, M.; Halim, W.; Ouaskit, S. Ethylene glycol based silver nanoparticles synthesized by polyol process: Characterization and thermophysical profile. J. Mol. Liq. 2020, 310, 113229.
67. Walshe, J.; Carron, P.M.; McLoughlin, C.; McCormack, S.; Doran, J.; Amarandei, G. Nanofluid Development Using Silver Nanoparticles and Organic-Luminescent Molecules for Solar-Thermal and Hybrid Photovoltaic-Thermal Applications. Nanomaterials 2020, 10, 1201.

68. Contreras, E.M.C.; Oliveira, G.A.; Filho, E.P.B. Experimental analysis of the thermohydraulic performance of graphene and silver nanofluids in automotive cooling systems. Int. J. Heat Mass Transf. 2019, 132, 375–387.
69. Selvam, C.; Irshad, E.C.M.; Lal, D.M.; Harish, S. Convective heat transfer characteristics of water–ethylene glycol mixture with silver nanoparticles. Exp. Therm. Fluid Sci. 2016, 77, 188–196.
70. Wu, X.; Chen, X.; Jin, S.; He, G.; Guo, Y.; Fang, W. Highly stable macroinitiator/platinum/hydrocarbon nanofluids for efficient thermal management in hypersonic aircraft from synergistic catalysis. Energy Convers. Manag. 2019, 198, 111797.
71. Wu, X.; Ye, D.; Jin, S.; Guo, Y.; Fang, W. Cracking of platinum/hydrocarbon nanofluids with hyperbranched polymer as stabilizer and initiator. Fuel 2019, 255, 115782.
72. Carrillo-Berdugo, I.; Midgley, S.D.; Grau-Crespo, R.; Zorrilla, D.; Navas, J. Understanding the Specific Heat Enhancement in Metal-Containing Nanofluids for Thermal Energy Storage: Experimental and Ab Initio Evidence for a Strong Interfacial Layering Effect. ACS Appl. Energy Mater. 2020, 3, 9246–9256.
73. Carrilo-Berdugo, I.; Estellé, P.; Sani, E.; Mercatelli, L.; Grau-Crespo, R.; Zorrila, D.; Navas, J. Optical and Transport Properties of Metal−Oil Nanofluids for Thermal Solar Industry: Experimental Characterization, Performance Assessment, and Molecular Dynamics Insights. ACS Sustain. Chem. Eng. 2021, 9, 4194–4205.
74. Qin, X.; Yang, S.; Chen, Y.; Qin, X.; Zhao, J.; Fang, W.; Luo, D. Thermal Conductivity and Stability of Hydrocarbon-Based Nanofluids with Palladium Nanoparticles Dispersed by Modified Hyperbranched Polyglycerol. ACS Omega 2020, 5, 31156–31163.
75. Cruz, C.C.R.; Da Silva, N.P.; Castilho, A.V.; Favre-Nicolin, V.A.; Cesar CLOrlande, H.R.B.; Dos Santos, D.S. Synthesis, characterization and photothermal analysis of nanostructured hydrides of Pd and PdCeO2. Sci. Rep. 2020, 10, 17561.
76. Yue, L.; Wub, J.; Gonga, Y.; Fang, W. Thermodynamic properties and pyrolysis performances of hydrocarbon-fuel-based nanofluids containing palladium nanoparticles. J. Anal. Appl. Pyrolysis 2016, 120, 347–355.
77. Patil, V.S.; Patil, S.H.; Patil, K.R.; Rode, C.V.; Coronas, A.; Nieto de Castro, C.A. Study of anion effect and heat transfer properties of Ru Ionanofluid. In Proceedings of the Solar Absorption Refrigeration Systems Operating with Ionic Liquids, an Indo-Spanish Workshop, IIT MADRAS, Chennai, India, 21–22 February 2014.
78. Bonet, F.; Delmas, V.; Grugeon, S.; Urbina, R.H.; Silvert, P.Y.; Tekaia-Elhissen, K. Synthesis of monodisperse Au, Pt, Pd, Ru and Ir nanoparticles in ethylene glycol. Nanostruct. Mater. 1999, 11, 1277–1284.

79. Zhang, T.; Li, S.-C.; Zhu, W.; Ke, J.; Yu, J.-W.; Zhang, Z.-P.; Dai, L.-X.; Gu, J.; Zhang, Y.-W. Iridium ultrasmall nanoparticles, worm-like chain nanowires, and porous nanodendrites: One-pot solvothermal synthesis and catalytic CO oxidation activity. Surf. Sci. 2016, 648, 319–327.
80. Santacruz, L.; Donnici, S.; Granados, A.; Shafir, A.; Vallribera, A. Fluoro-tagged osmium and iridium nanoparticles in oxidation reactions. Tetrahedron 2018, 74, 6890–6895.
81. Tanaka, H.; Orita, K.; Maede, A.; Ishikawa, H.; Miura, M.; Arai, S.; Higushi, T.; Otha, S.; Muto, S. Dynamics of Rh nanoparticle surface structure during NO reduction revealed by operando transmission electron microscopy. Appl. Catal. A Gen. 2021, 626, 118334.
82. Swiatkowska-Warkocka, Z. Bimetal CuFe Nanoparticles—Synthesis, Properties, and Applications. Appl. Sci. 2021, 11, 1978.
83. Zhou, G.; Lu, M.; Yang, Z. Aqueous Synthesis of Copper Nanocubes and Bimetallic Copper/Palladium Core−Shell Nanostructures. Langmuir 2006, 22, 5900–5903.
84. Behera, A.; Mittu, B.; Padhi, S.; Patra, N.; Singh, J. Chapter 25—Bimetallic nanoparticles: Green synthesis, applications, and future perspectives. In Multifunctional Hybrid Nanomaterials for Sustainable Agri-Food and Ecosystems, Micro and Nano Technologies; Elsevier: Amsterdam, The Netherlands, 2020; pp. 639–682.
85. Loza, K.; Heggen, M.; Epple, M. Synthesis, Structure, Properties, and Applications of Bimetallic Nanoparticles of Noble Metals. Adv. Funct. Mater. 2020, 30, 1909260.
86. Singh, S.K.; Iizuka, Y.; Xu, Q. Nickel-palladium nanoparticle catalyzed hydrogen generation from hydrous hydrazine for chemical hydrogen storage. Int. J. Hydrogen Energy 2011, 36, 11794–11801.
87. Feng, R.; Li, M.; Liu, J. Synthesis of core–shell Au@Pt nanoparticles supported on Vulcan XC-72 carbon and their electrocatalytic activities for methanol oxidation. Colloids Surf. A 2012, 406, 6–12.
88. Kumari, M.; Jacob, J.; Philip, D. Green synthesis and applications of Au-Ag bimetallic nanoparticles. Spectrochim. Acta Part A Mol. Biomol. Spectrosc. 2015, 137, 185–192.
89. Hammami, I.; Alabdallah, N.M.; Jomaa, A.A.; Kamoun, M. Gold nanoparticles: Synthesis properties and applications. J. King Saud Univ. Sci. 2021, 33, 101560.
90. Gad, G.M.A.; Hegazy, M.A. Optoelectronic properties of gold nanoparticles synthesized by using wet chemical method. Mater. Res. Express 2019, 6, 085024.
91. Jan, H.; Gul, R.; Andleeb, A.; Ullah, S.; Shah, M.; Khanum, M.; Ullah, I.; Hano, C.; Abbasi, B.H. A detailed review on biosynthesis of platinum nanoparticles (PtNPs), their potential antimicrobial and biomedical applications. J. Saudi Chem. Soc. 2021, 25, 101297.

92. Ledendecker, M.; Paciok, P.; Osowiecki, W.T.; Pander, M.; Heggen, M.; Göhl, D.; Kamat, G.A.; Erbe, A.; Mayrhofer, K.J.; Alivisatos, A.P. Engineering gold-platinum core-shell nanoparticles by self-limitation in solution. Commun. Chem. 2022, 5, 71.
93. Lucas, G.L.L.; Romanus, H.; Ispas, A.; Bund, A. Hollow platinum-gold and palladium-gold nanoparticles: Synthesis and characterization of composition-structure relationship. J. Nanopart. Res. 2022, 24, 245.
94. Wang, S.-S.; Wu, C.-W.; Chen, P.-Y.; Lee, C.-L. Preferential deposition of gold and platinum atom on palladium nanocubes as catalysts for oxidizing glucose in the phosphate-buffered solution. J. Electroanal. Chem. 2023, 930, 117142.
95. Lou, Z.; Fujitsuka, M.; Majima, T. Pt–Au triangular nanoprisms with strong dipole plasmon resonance for hydrogen generation studied by single-particle spectroscopy. ACS Nano 2016, 10, 6299–6305.
96. Zhang, H.; Toshima, N. Synthesis of Au/Pt bimetallic nanoparticles with a Pt-rich shell and their high catalytic activities for aerobic glucose oxidation. J. Colloid Interface Sci. 2013, 394, 166–176.
97. Mallah, A.R.; Zubir, M.N.M.; Alawi, O.A.; Newaz, K.S.; Badry, A.B.M. Plasmonic nanofluids for high photothermal conversion efficiency in direct absorption solar collectors: Fundamentals and applications. Sol. Energy Mater. Sol. Cell. 2019, 201, 110084.
98. Verma, A.K.; Yadav, N.; Sing, S.P.; Dey, K.K.; Singh, D.; Yadav, R.R. Study of Ultrasonic Attenuation and Thermal Conduction in Bimetallic Gold/Platinum Nanofluids. Johnson Matthey Technol. Rev. 2021, 65, 556–567.
99. Chen, M.; He, Y.; Zhu, J. Preparation of Au–Ag bimetallic nanoparticles for enhanced solar photothermal conversion. Int. J. Heat Mass Transf. 2017, 114, 1098–1104.
100. Zhu, G.; Wang, L.; Bing, N.; Xie, H.; Yu, W. Enhancement of photothermal conversion performance using nanofluids based on bimetallic Ag-Au alloys in nitrogen-doped graphitic polyhedrons. Energy 2019, 183, 747–755.
101. Sánchez-Ramírez, J.F.; Jiménez Pérez, J.L.; Cruz Orea, A.; Gutiérrez Fuentes, R.; Bautista-Hernández, A.; Pal, U. Thermal diffusivity of nanofluids containing Au/Pd bimetallic nanoparticles of different compositions. J. Nanosci. Nano-Technol. 2006, 63, 685–690.
102. Gutierrez Fuentes, R.; Pescador Rojas, J.A.; Jiménez-Pérez, J.L.; Sanchez Ramirez, J.F.; Cruz-Orea, A.; Mendoza-Alvarez, J.G. Study of thermal diffusivity of nanofluids with bimetallic nanoparticles with Au(core)/Ag(shell) structure. Appl. Surf. Sci. 2008, 255, 781–783.
103. Dsouza, A.; Shilpa, M.P.; Gurumurthy, S.C.; Nagaraja, B.S.; Mundinamani, S.; Raman, K.; Gedda, M.; Murari, M.S. CuAg and AuAg bimetallic nanoparticles for catalytic and heat transfer applications. Clean Technol. Environ. Policy 2021, 23, 2145–2155.

104. Makishima, A. Possibility of hybrids materials. Ceram. Jpn. 2004, 39, 90–91.
105. Gamachu, D.; Ibrahim, W. Mixed convection flow of viscoelastic Ag-Al2O3/water hybrid nanofluid past a rotating disk. Phys. Scr. 2021, 96, 125205.
106. Hayat, T.; Nadeem, S. Heat transfer enhancement with Ag–CuO/water hybrid nanofluid. Results Phys. 2017, 7, 2317–2324.
107. Singh, J.P.; Nandi, T.; Ghosh, S.K. Structure-property relationship of silver decorated functionalized reduced graphene oxide based nanofluids: Optical and thermophysical aspects and applications. Appl. Surf. Sci. 2021, 542, 148410.
108. Naderi, A.; Gazori, H.; Bozegi, M. Experimental Analysis PVP Coated Silver Nanofluid Properties for Application in Photovoltaic/Thermal (PVT) Collectors. J. Model Based Res. 2020, 1, 28–40.
109. Mbambo, M.C.; Madito, M.J.; Khamliche, T.; Mtshali, C.B.; Khumalo, Z.M.; Madiba, I.G.; Mothudi, B.M.; Maaza, M. Thermal conductivity enhancement in gold decorated graphene nanosheets in ethylene glycol based nanofluid. Sci. Rep. 2020, 10, 14730.
110. Yarmand, H.; Gharehkhani, S.; Shirazi, S.F.S.; Goodarzi, M.; Amiri, A.; Sarsam, W.S.; Alehashem, M.S.; Dahari, M.; Kazi, S.N. Study of synthesis, stability and thermo-physical properties of graphene nanoplatelet/platinum hybrid nanofluid. Int. Commun. Heat Mass Transf. 2016, 77, 15–21.
111. Wang, L.; Zhu, G.; Shen, L.; Yu, W.; Zhu, D.; Zhang, Y.; Zhang, L.; Xie, H. Enhanced solar energy absorption on nitrogen-doped carbon nanotubes decorated with gold-palladium bimetallic nanoparticles. Therm. Sci. 2018, 22, S701–S708.
112. Jaiswal, A.K.; Wan, M.; Singh, S.; Singh, D.K.; Yadav, R.R.; Singh, D.; Mishra, G. Experimental Investigation of Thermal Conduction in Copper-Palladium Nanofluids. J. Nanofluids 2016, 5, 496–501.
113. Aberoumand, S.; Jafarimoghaddam, A. Tungsten (III) oxide (WO3)—Silver/transformer oil hybrid nanofluid: Preparation, stability, thermal conductivity and dielectric strength. Alex. Eng. J. 2018, 57, 169–174.
114. Ma, M.; Zhai, Y.; Yao, P.; Li, Y.; Wang, H. Effect of surfactant on the rheological behavior and thermophysical properties of hybrid nanofluids. Powder Technol. 2021, 379, 373–383.
115. Li, H.; He, Y.; Wang, C.; Wang, X.; Hu, Y. Tunable thermal and electricity generation enabled by spectrally selective absorption nanoparticles for photovoltaic/thermal applications. Appl. Energy 2019, 236, 117–126.
116. Hjerrild, N.E.; Mesgari, S.; Crisostomo, F.; Scott, J.A.; Amal, R.; Taylor, R.A. Hybrid PV/T enhancement using selectively ab-sorbing Ag–SiO2/carbon nanofluids. Sol. Energy Mater. Sol. Cells 2016, 147, 282–287.

117. Munkhbayar, B.; Tanshen, M.R.; Jeoun, J.; Chung, H.; Jeong, H. Surfactant-free dispersion of silver nanoparticles into MWCNT-aqueous nanofluids prepared by one-step technique and their thermal characteristics. Ceram Int. 2013, 39, 6415–6425.
118. Baby, T.T.; Ramaprabhu, S. Synthesis and nanofluid application of silver nanoparticles decorated graphene. J. Mater. Chem. 2011, 21, 9702–9709.
119. Chen, L.; Yu, W.; Xie, H. Enhanced thermal conductivity of nanofluids containing Ag/MWNT composites. Powder Technol. 2012, 231, 18–20.
120. Botha, S.S.; Ndungu, P.; Bladergroen, B.J. Physicochemical properties of oil-based nanofluids containing hybrid structures of silver nanoparticles supported on silica. Ind. Eng. Chem. Res. 2011, 50, 3071–3077.
121. Han, W.S.; Rhi, S.H. Thermal characteristics of grooved heat pipe with hybrid nanofluids. Therm. Sci. 2011, 15, 195–206.
122. Dinarvand, S.; Rostami, M.N. An innovative mass-based model of aqueous zinc oxide–gold hybrid nanofluid for von Kármán´s swirling flow. J. Therm. Anal. Calorim. 2019, 138, 845–855.
123. Jin, X.; Lin, G.; Zeiny, A.; Jin, H.; Bai, L.; Wen, D. Solar photothermal conversion characteristics of hybrid nanofluids: An ex-perimental and numerical study. Renew. Energy 2019, 141, 937–949.
124. Baniamerian, Z.; Mashayekhi, M.; Mehdipour, R. Evaporative Behavior of Gold-Based Hybrid Nanofluids. J. Thermo-Phys. Heat Transf. 2017, 32, 284–291.